AFRL-RX-WP-TR-2011-4151

NANOTECHNOLOGY-ENHANCED LUBRICANTS FOR RF MEMS SWITCHES

Daniel J. Hyman
XCOM Wireless, Inc.

Steven D. Patton
Univ. Dayton Research Inst.

March 2011
Final Report

AIR FORCE RESEARCH LABORATORY
MATERIALS AND MANUFACTURING DIRECTORATE
WRIGHT-PATTERSON AIR FORCE BASE, OH 45433-7750
AIR FORCE MATERIEL COMMAND
UNITED STATES AIR FORCE

NOTICE AND SIGNATURE PAGE

Using Government drawings, specifications, or other data included in this document for any purpose other than Government procurement does not in any way obligate the U.S. Government. The fact that the Government formulated or supplied the drawings, specifications, or other data does not license the holder or any other person or corporation; or convey any rights or permission to manufacture, use, or sell any patented invention that may relate to them.

This report was cleared for public release by the Wright-Patterson Air Force Base (WPAFB) Public Affairs Office and is available to the general public, including foreign nationals. Copies may be obtained from the Defense Technical Information Center (DTIC) (http://www.dtic.mil).

AFRL-RX-WP-TR-2011-4151 HAS BEEN REVIEWED AND IS APPROVED FOR PUBLICATION IN ACCORDANCE WITH THE ASSIGNED DISTRIBUTION STATEMENT.

*//signature//

PATRICK S. CARLIN, Project Engineer
Nanostructured & Biological Materials Branch
Nonmetallic Materials Division

//signature//

RICHARD A. VAIA, Acting Chief
Nanostructured & Biological Materials Branch
Nonmetallic Materials Division

//signature//

SHASHI SHARMA, Deputy Division Chief
Nonmetallic Materials Division
Materials and Manufacturing Directorate

This report is published in the interest of scientific and technical information exchange, and its publication does not constitute the Government's approval or disapproval of its ideas or findings.

*Disseminated copies will show "//signature//" stamped or typed above the signature blocks.

REPORT DOCUMENTATION PAGE

Form Approved
OMB No. 0704-0188

1. REPORT DATE *(DD-MM-YY)*	2. REPORT TYPE	3. DATES COVERED *(From - To)*
March 2011	Final	23 October 2008 – 31 March 2011

4. TITLE AND SUBTITLE
NANOTECHNOLOGY-ENHANCED LUBRICANTS FOR RF MEMS SWITCHES

5a. CONTRACT NUMBER
FA8650-09-C-5041

5b. GRANT NUMBER

5c. PROGRAM ELEMENT NUMBER
62102F

6. AUTHOR(S)
Daniel J. Hyman XCOM Wireless, Inc.
Steven D. Patton Univ. Dayton Research Inst.

5d. PROJECT NUMBER
4347

5e. TASK NUMBER
ML

5f. WORK UNIT NUMBER
BP112100-B

7. PERFORMING ORGANIZATION NAME(S) AND ADDRESS(ES)
XCOM Wireless, Inc.
2815 Junipero Ave., #110
Signal Hill, CA 90755

8. PERFORMING ORGANIZATION REPORT NUMBER

9. SPONSORING/MONITORING AGENCY NAME(S) AND ADDRESS(ES)
Air Force Research Laboratory
Materials and Manufacturing Directorate
Wright-Patterson Air Force Base, OH 45433-7750
Air Force Materiel Command
United States Air Force

10. SPONSORING/MONITORING AGENCY ACRONYM(S)
AFRL/RXBN

11. SPONSORING/MONITORING AGENCY REPORT NUMBER(S)
AFRL-RX-WP-TR-2011-4151

12. DISTRIBUTION/AVAILABILITY STATEMENT
Approved for public release; Distribution unlimited.

13. SUPPLEMENTARY NOTES
Report contains color. Case Number 88ABW-2011-2394 (RX11-0439); Clearance Date: 29 Apr 2011.

14. ABSTRACT *(Maximum 200 words)*
This program was to develop a nanoparticle lubricant (NPL) technology capable of improving noble metal Ohmic contact RF MEMS switching circuit power handling and lifetime ratings to meet tactical radio requirements. A candidate NPL was identified early in the program, with a manufacturing process developed by the Univ. of Dayton Research Institute. A deposition process was developed for compatibility with a production MEMS assembly line. Noble-alloy MEMS relays were tested for hot-switch and cold-switch lifetime at 5 mW and 2 W of continuous wave RF power at 50 Ohms. The relays without NPL performed as expected, within the predicted control performance already characterized for the components. The relays with NPL showed improved lifetime, from approximately 2x for cold-switched conditions, up to nearly 10x for high power hot-switched conditions. While this improvement was less than the 100x demonstrated in initial laboratory tests, the 10x improvement was a critical leap forward for MEMS technology. The engineering sacrifice was on ultra-low-load repeatability, which was not as good with the NPL material, but this specification does not have a strict requirement for tactical radio applications. Finally, a demonstration amplifier validated the tuning circuit concept with 1-2 dB of gain improvement.

15. SUBJECT TERMS
RF MEMS, switch, relay, nanoparticle, lubrication, nanotechnology, power handling

16. SECURITY CLASSIFICATION OF:			17. LIMITATION OF ABSTRACT:	18. NUMBER OF PAGES	19a. NAME OF RESPONSIBLE PERSON (Monitor)
a. REPORT	b. ABSTRACT	c. THIS PAGE			Patrick Carlin
Unclassified	Unclassified	Unclassified	SAR	64	19b. TELEPHONE NUMBER *(Include Area Code)* (937) 255-9162

Table of Contents

Section **Page**

List of Figures

Figure **Page**

List of Figures (Continued)

Figure **Page**

List of Tables

Table **Page**

1. Summary

XCOM Wireless (XCOM) is a developer of Microfabricated ElectroMechanical Systems (MEMS) for next generation Radio Frequency (RF) test equipment and adaptive radios. The University of Dayton Research Institute (UDRI) and the Air Force Research Laboratory (AFRL) had developed a nanoparticle lubricant (NPL) material that demonstrated substantial switching performance benefits in laboratory experiments. The hot-switch survivability and lifetime of RF MEMS relays does not presently meet Air Force radio requirements, so marked improvement in that specification is highly desirable to enable these advanced technologies to be deployed.

This program's objectives were to modify the NPL material for compatibility with the XCOM RF MEMS devices and packaging processes, then develop a method of deposition and test its performance directly. The goal is to quantify the performance gains that can be obtained by adding the new NPL material to a production part, and under what conditions those gains are greatest. In addition, a circuit-level demonstration of the value of RF MEMS was performed in order to justify the need for solving its hot-switch lifetime problem.

The program technical effort had three tasks:
1. Modify the UDRI/AFRL nanoparticle lubricant for compatibility with RF MEMS devices.
2. Implement the modified NPL into hybrid and wafer-packaged RF MEMS devices.
3. Demonstrate subsystem-level improvements using NPL and RF MEMS technologies.

In the first task and year of the program, UDRI worked through much iteration to modify the NPL material, manufacturing, and transport medium into a highly stable and pure product. The program over-ran time and funds starting with this task, but, ultimately, significant volumes of three concentrations of high-quality final material were delivered to XCOM for deposition experiments. The NPL compatibility modification task is considered a complete success.

In the second task, XCOM developed a deposition process compatible with the hybrid and wafer-scale packaging steps for RF MEMS relays, again requiring many iterations. Parts with NPL were assembled and tested next to control components using standard processes. The NPL enhanced relays showed marked improvement in switching lifetime, especially under hot-switch conditions (a critical focus), with improvement results summarized in Table 1, below.

Work relevant to the final task was performed by complementary research programs, including internal R&D funds. A MEMS-tunable power amplifier was designed and modeled, and a simplified prototype was tested to show high performance and reduced size relative to state-of-the-art products. The end product goal and future value of this research thrust is validated.

Table 1: Synopsis of critical relay performance improvement in this program

Specification	Conditions	Est. Baseline	**Baseline**	NPL Goal	**NPL**	Units	**Increase**
Cold Switched	at 33 dBm, 50 Ohm	10^7 to 10^8	**8x10^7**	~2x10^8	**1.4x10^8**	cycles	**~2x**
Cold Switched	at 7 dBm, 50 Ohm	10^8 to 10^9	**~7x10^8**	~1x10^9	**~1x10^9**	cycles	**~1x**
Warm Switched	at 7 dBm, 50 Ohm	10^4 to 10^5	**4x10^5**	~1x10^7	**7x10^5**	cycles	**~2x**
Hot Switched	at 33 dBm, 50 Ohm	10^2 to 10^4	**5x10^4**	~1x10^5	**2x10^5**	cycles	**~5x (!!)**

2. Introduction

This program addresses the increasing complexity of multi-waveform radio electronics, which is a critical Air Force problem. An examination of present tactical C4ISR interoperability exposes a critical need for improved RF components and subsystems for the tactical warfighter. At its essence, the goal for this program is to combine two emerging technologies in a complementary manner to create one of these critical next-generation components. With the technologies developed in this program, future radios can be made smaller and more power efficient, last longer in the field, and have greater capabilities.

2.1. Problem Background

The Air Force employs numerous communication links between space-borne assets, airborne platforms, ground forces, and unattended ground sensors (UGS), all platforms that are sensitive to size, weight, and power. Increasing bandwidth and situational awareness through dependable data access has continuously enhanced force asymmetry. More waveform support and radio adaptability is needed for redundancy, compatibility, and bandwidth on demand, especially as sensor platforms proliferate and capabilities increase. Unfortunately, increased radio complexity dramatically increases size, weight, power consumption, and cost. Additional power is wasted and heat is generated because antennas and amplifiers cannot adapt to changing radio conditions. Next-generation tuners, filter modules, and amplifiers are needed to "dial back" the size, weight, and power of these more complex radios (JTRS, CSR, Soldier Radio, WIN-T, etc.).

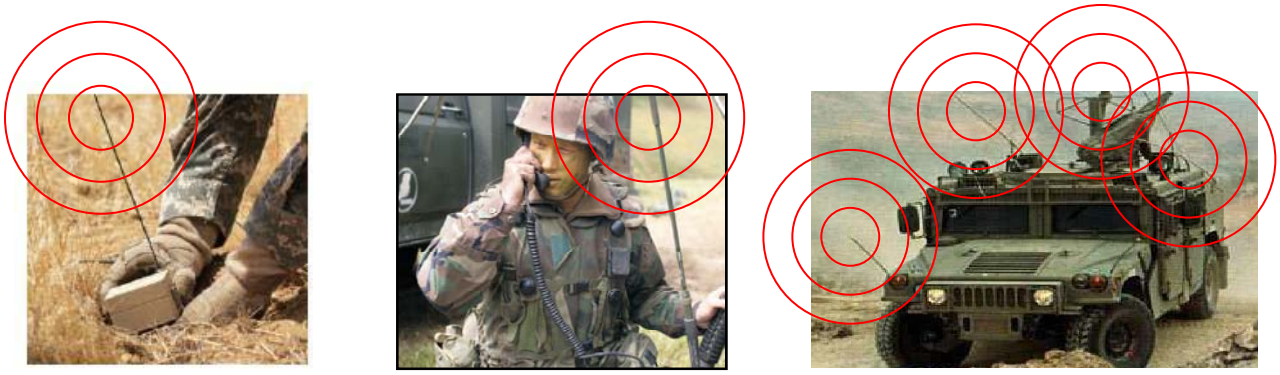

Figure 1: Harris Falcon Watch™ sensors, Falcon™ radios, and growing multi-band problem.

One of the next-generation wide-band technologies for low-loss tunable RF circuits is Microfabricated ElectroMechanical Systems (MEMS). RF MEMS have higher linearity, bandwidth, repeatability, ruggedness, and lower loss than the most advanced solid-state switches. Unfortunately, they do not have the warm-switching and hot-switching power survivability required by Government radios, and require improvement before these incredible components can be fielded. An important background detail is the difference between the types of switching, as these are critical metrics for switching and tuning technologies in the radio community.

Cold-switched operation refers to power passing through contacts only when state changes have been completed, and a device is open or closed. About 90% of all switching across all wireless applications either is or can be performed cold-switched. The majority of applications require a moderate lifetime of operation at rated power, typically between 10M and 10B. The rating is

dependent on the function as well as on the platform (i.e., munitions, unattended ground sensor, terrestrial, UAV, or flight platform). A typical example for an adaptive tuning circuit in a filter or amplifier would have cold-switched lifetime of 1B cycles at 5W at 50 or 100 Ohms. The actual power levels in use will conform to a usage envelope, as will the localized impedance, so any test or specification will be at relevant equivalent or worst-case conditions. High-lifetime programs (e.g., DARPA MEMS Improvement Program) have resulted in heroic research efforts, but there are in actuality very few applications that require beyond 10B of rated cold-switched life, such as high-value space-borne assets with 12+ year horizons to deployment.

Warm-switched operation refers to load power passing through the contacts during state change, although this will be much lower than the rated power. More than 50% of RF switching in Defense applications must support warm switching, but this is much lower in consumer applications. This is a must-have for many multi-standard radios, and therefore a relevant area of R&D to support for Government applications. Typical warm-switching powers vary between 100 uW and 100 mW, depending on the circuit function and platform. The closer a component is to the antenna, rather than behind a switchplexer or circulator, the higher a received power level will be. Also, the more likely a platform will operate in proximity to radiators or noise sources (e.g., EW transmitters), the higher this will be. The survivability cycles will typically be in the range of 1M to 100M events, with lifetimes associated with different power levels.

Hot-switched operation refers to the presence of full/high rated load power passing through the contacts during state change. Very few Defense applications require hot-switching of any kind. This program is not intended to concentrate on hot-switching, although it is recognized that improvements in warm switching are likely to also result

XCOM has made considerable strides in maturing RF MEMS in recent years, as can be seen by the meeting of nearly all RF, electromechanical, and ruggedness requirements of Air Force radios. Unfortunately, the technical requirements for ***hot-switching*** demanded by these radio applications are still beyond the performance of *any* low-loss device by *any* developer according to Harris, General Dynamics, Boeing, Raytheon, Teledyne, Motorola, BAE, Smiths, and others. All have demand improvements according to the following table.

2.2. State-Of-The-Art

XCOM Wireless (XCOM) has one of the few commercially available Ohmic-contact MEMS relays (four-terminal switching devices) in the world. XCOM MEMS relays are based on a microscopic mechanical switching element. These have a low loss (<0.25 Ohm) suitable for tuning and filter applications, which very few developers have achieved. These devices are extremely rugged, with good speed and power handling, and moderate lifetime, suitable for tuning and mode-switching applications.

The University of Dayton Research Institute (UDRI) has a highly advanced nanotechnology-enabled heterogeneous lubricant film that is highly complementary and overcomes a critical limitation. A brief overview of the background state of the art in these technologies is provided below, with Technology Readiness Level (TRL) details provided in Appendix A.

Figure 2: XCOM RF MEMS switching element and S-parameters of relay die.

Below is a table of Air Force requirements contrasted with initial XCOM MEMS performance. These requirements are not necessarily "best of breed" of each specification as reported by developers who favor one in lieu of another. These are instead selected to meet the actual needs of a wide and relevant range of Defense applications that RF MEMS are well suited for. Specifications not mentioned (power consumption, linearity, etc.) have already been well-met and were not a focus of this program.

Table 2: Performance specifications of typical Defense radio applications.

Specification	Conditions	Now Min	Now Max	Goal Min	Goal Max	Units
Bandwidth	-15 dB input refl.	**0**	**20000**	30	12000	MHz
Loss	in band	**0.1**	0.3	**0.05**	**0.2**	dB
Repeatability	deviation from typ. loss	**0.02**			0.05	dB
Isolation	in band (negative)	**30**	**60**	30	60	-dB
Speed – Off	to rated isolation	**0.4**	**3**		6 (2 best)	usec
Speed – On	predictive, to rated loss	**4**	8		**6** (2 best)	usec
Speed – On	reactionary, to rated loss	**30**	50		**40** (10 best)	usec

In the table above, XCOM RF MEMS (Now Min and Now Max columns) already met the majority of the RF and electromechanical requirements for these applications (Goal Min and Goal Max columns). Bold Goal values are barely met under some circumstances, but not met under other operating conditions, etc. The work in this program must be sensitive not to fail any of these requirements, or make borderline requirements worse.

UDRI had developed a nanotechnology that showed the potential to improve power handling of RF MEMS switches and relays, which is a critical metric where the XCOM components do not meet requirements. Nanoparticle liquids (NPLs) are monolithic hybrid materials comprised of an inorganic nanometer-sized metallic core and an organic low viscosity corona. As a contact lubricant, NPLs provide controlled nanotexturing, a high conductivity of metallic nanoparticles, and a limited liquidity for lubricant reflow to damaged areas. Particle size varied from about 15 nm to 25 nm, each surrounded by a 1.5-2 nm corona of ionic liquid. A scanning electron micrograph (SEM) of a gold electrode spin-coated with a gold-based NPL is shown below.

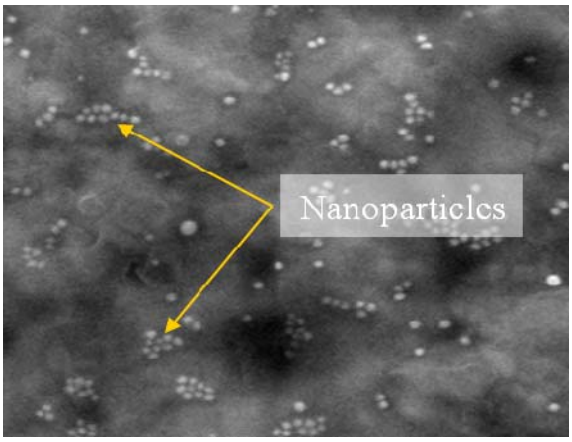

Figure 3: SEM image of an Au electrode spin-coated with an Au nanoparticle liquid.

Below is shown a transmission electron microscope (TEM) image and schematic of an example gold-based NPL. The anion is mercaptoethanesulfonate ($HSCH_2CH_2SO_3^-$), and the cat-ion is quaternary ammonium ($CH_3N^+R_3$), where R=C_{10}-C_{12}. Mercaptoethanesulfonate (MES) forms a covalent bond with the Au nanoparticle by S-H bond breaking (thiol-Au chemistry), and quaternary ammonium bonds ionically to the MES sulfonate group and completes the structure. Quaternary ammonium was chosen in part because of its long hydrocarbon chains and branch structure that prevent agglomeration and promote liquidity (it flows to coat MEMS structures).

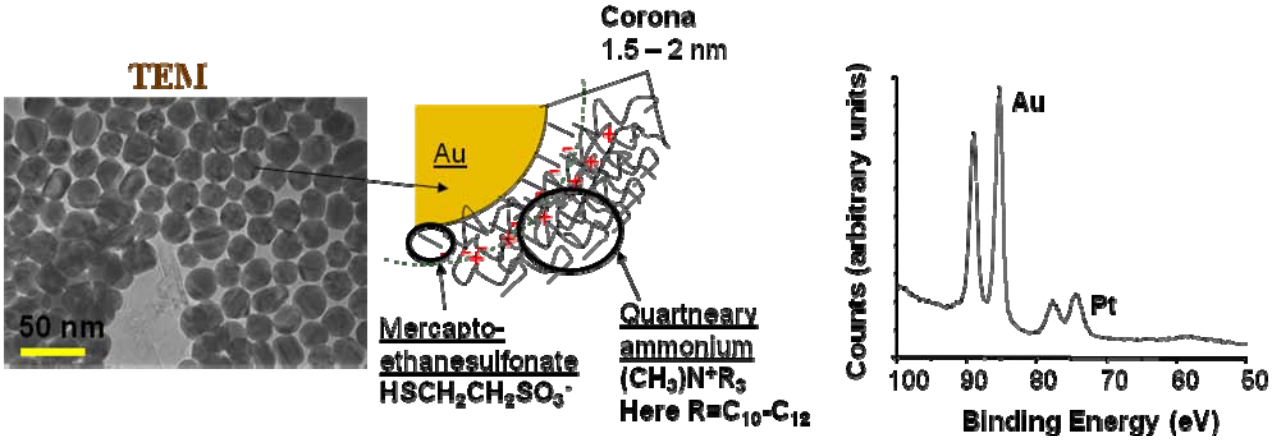

Figure 4: Gold nanoparticles with ionic liquid corona, and XPS of bimetal Au-Pt NPL.

Initial studies suggested that nanoparticles (NPs) and NPLs may extend the lifetime of RF MEMS switches in hot-switching applications. Key mechanisms for improved performance and durability are small radii of curvature of nanoscopic asperities, surface morphology that spreads current through nanoasperity contacts, and lubricant replenishment. Essentially, electrical contact was "cleaner when you make it, and heats less when you break it." Initial tests had shown that an increase in hot-switch lifetime at low to moderate DC loads (0.01-1 mA) were increased by 10x to 1000x and more in a laboratory environment using NPL lubricants. These early demonstrated levels of hot-switch improvement would enable the XCOM RF MEMS device to meet the requirements of Government radio contractors, and it was surmised that even further improvement with bimetal nanoparticles would be possible.

3. Methods, Assumptions, and Procedures

This program was developed starting from baseline technologies with their own methods and procedures of manufacture, adding clear program objectives and decision trees for how to merge these technologies together to solve the Air Force radio front end problem. The objectives and task plan for accomplishing the program are repeated here as paraphrased from the original proposal with initial performance metrics and goals in the following table:

Table 3: Specification status and initial program goals.

Specification	Conditions	Now Min	Now Max	Goal Min	Units
Cold Switched	at 30 dBm, 50 Ohm	10^8	**10^9**	10^9	cycles
Cold Switched	at 40 dBm, 50 Ohm	10^4	10^6	**10^8**	cycles
Warm Switched	at 0 dBm, 50 Ohm	10^5	10^7	**10^8**	cycles
Warm Switched	at 10 dBm, 50 Ohm	10^4	10^6	**10^7**	cycles
Hot Switched	at 20 dBm, 50 Ohm	10^3	10^5	**10^6**	cycles
Hot Switched (desired)	at 40 dBm, 50 Ohm	0	0	**10^2**	cycles

As can be seen, the XCOM devices did not meet warm and hot-switching requirements by about 10-100x, which is a critical technical impediment to our ability to field these powerful high-performance devices. The overall goal of this program was to improve hot-switch power handling lifetime of XCOM switching elements without sacrificing other performance metrics.

3.1. Program Objectives

The improvement of warm-switch power handling is the most important aspect of this program The following six objectives formed the basis for the tasks detailed in the proposal. The goal was to increase the readiness level of a suite of SBIR technologies up to TRL5-6 and MRL2 towards future insertion in Government radios.

1. **Identify** appropriate nanotechnology-enhanced lubricant films that are compatible with the XCOM packaging process and with the RF MEMS switching devices.
2. **Modify** (if necessary) the present particle additives and/or liquid chemistries to enhance performance and/or compatibility with XCOM RF MEMS devices.
3. **Demonstrate** that hybrid-packaged RF MEMS relay products can be enhanced to meet radio hot-switch power handling and lifetime requirements without sacrificing resistance.
4. **Transition** a lubricant film from the laboratory environment into the manufacturing environment with XCOM for hybrid-packaged and/or wafer-scale packaged devices.
5. **Develop** an impedance matching circuit using the standard RF MEMS switching devices from the relay product, and that employing the selected lubricant film(s).
6. **Quantify** circuit-level improvements in amplifier efficiency using the impedance matching circuit

3.2. Program Task Overview

In brief, the Air Force problem addressed is the increasing complexity of multi-waveform radio electronics, with the goal of enabling future radios that can be made smaller, more efficient, and to last longer in the field with greater capabilities. The six technical objectives and performance requirements are organized into tasks and subtasks to merge RF MEMS and NPL technologies to address a broad spectrum of real needs of Air Force radio developers.

3.2.1. Task Flow Chart

The effort has three tasks, which address the primary lubricant and MEMS platform technologies, then implement them in a highly desirable circuit demonstration. The tasks are:

1. Develop nanoparticle lubricant, using existing UDRI NPL fluids first, then modifying it as needed for enhanced compatibility with RF MEMS relay manufacturing.
2. Implement the NPL in MEMS, using existing hybrid XCOM relays, then demonstrating suitability for future wafer-scale packaging.
3. Demonstrate improved power efficiency, modifying an XCOM tuning circuit to implement an NPL, then quantifying improvements in output and efficiency.

Each Task included Subtasks, representing a labor division for monitoring of technical progress, and allowing greater control in terms of gating milestones and decision making. Subtask dependency, coordination, and critical paths were graphically presented below with technology decisions and gating details provided in the detailed descriptions to follow. Prerequisites are shown below by arrows in and dependent Subtasks shown by arrows out.

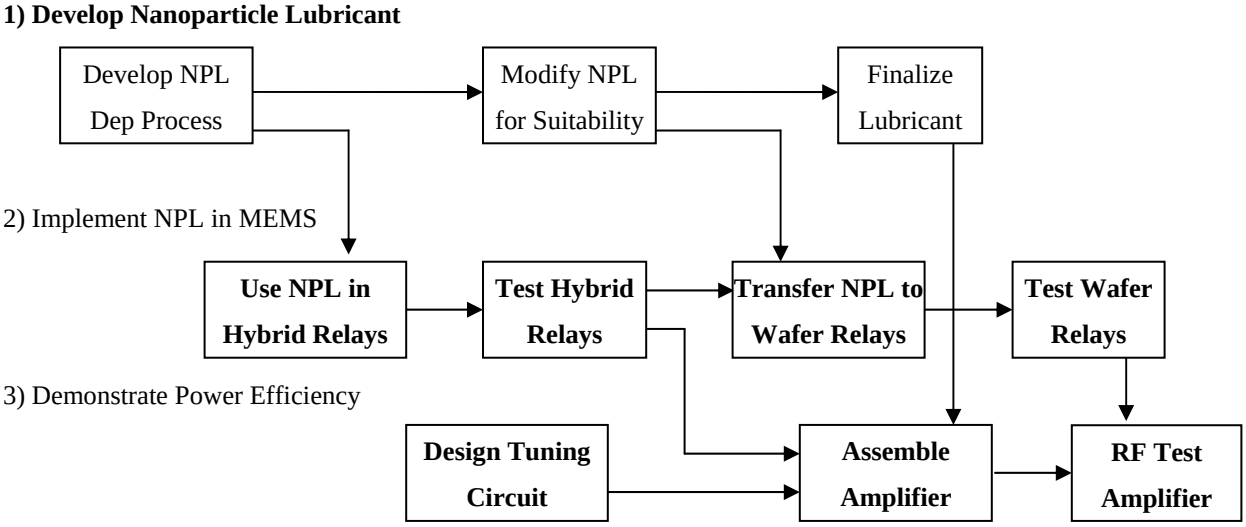

Figure 5: Program Subtask flow chart showing dependency of NPL and MEMS development efforts.

3.2.2. Task Decision Tree

The diagram right illustrates the most relevant technical questions of this program, and shows the iterative nature of NPL development with MEMS devices. There are three likely valuable benefits that can result from this work. If any is successful, then a viable RF MEMS-based NPL-enhanced product can result. This program was (and still is) therefore highly likely to further valuable applied research.

The first anticipated benefit was to demonstrate that an XCOM RF MEMS relay can be combined with NPL in a hybrid package (present form) with a substantive hot-switch advantage. This alone could enable a desirable switch matrix product to begin Government radio qualification.

The second area of anticipated benefit was a potential improvement that NPL has on ultra-low load repeatability. This is critical for many radar and communication test equipment, and is a high-value added feature for the relay product line XCOM is releasing for the industrial test equipment market.

The third benefit towards a potential product line is with improved efficiency for tuning circuits. This is of interest to many Government and civilian radio developers, and would greatly enhance the dominance of U.S. communications companies in the area of adaptive and cognitive radios.

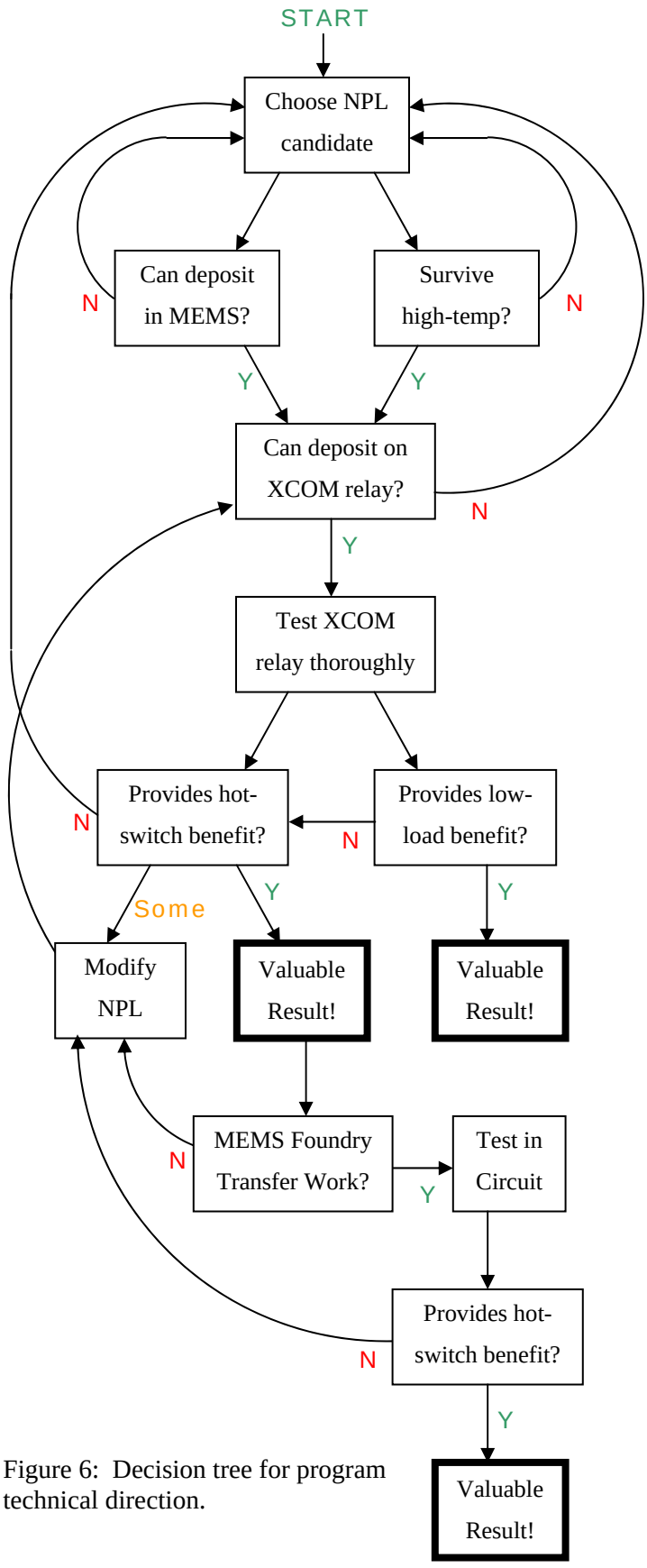

Figure 6: Decision tree for program technical direction.

3.3. Program Task Procedures

The following details the three major technical tasks of this program. Task 1 addressed the application, testing, and refinement of nanoparticle liquid (NPL) lubricant layers. Task 2 addressed the compatibility of these NPL layers with XCOM RF MEMS hybrid and wafer-scale packaging processes, and assesses their performance improvements. Task 3 was to create a tuned amplifier prototype of considerable interest to Government radio developers, using the NPL-augmented MEMS devices for improved performance.

3.3.1. Task 1 – Develop Nanoparticle Lubricant

Task 1, Subtask A – Develop NPL Deposition Process

In this first Subtask, we were to develop methods to apply existing NPLs to XCOM MEMS devices during packaging. NPLs were initially successfully applied to comparatively featureless surfaces using both dip-coating and spin-coating from a toluene solution. It was hoped that, due to the low surface energy (flowability) of the solution, a set of process parameters for one of these two methods will be appropriate for coating RF MEMS contacts underneath existing microstructures which have a 2-3 micron gap for fluid flow.

An initial NPL deposition experiment for RF MEMS had already been performed, with a variant dip-method used to saturate the surface of a bare XCOM MEMS relay die. The volume of solution used was over 1000x that used in the UDRI experiments. Testing found 75% stuck-down MEMS and no change in contact resistance, matching findings from UDRI when "too much" NPL is used. SEM verified that nanoparticle clusters were too large to be effective, so a true deposition process was needed.

A valuable find, however, was that the NPL did deposit underneath the MEMS microstructure, specifically coating the lower electrode of the relay contacts. Also proven was that no shorting or electrostatic weakness was present in the over-coated devices, so NPL can coat all surfaces equally without degrading relay operation. Both of these are extremely encouraging with regards to process development and compatibility.

This subtask was to be more of the same type of work, but with considerably greater rigor using wafers as well as bare die. Existing NPLs were to be applied by various methods, and analyzed through microscopy techniques to determine what was deposited with quantified clustering. While underway, tests for packaging compatibility would be performed by inserting an NPL dip step into the existing XCOM hybrid packaging process. The parts were then to be dismantled and the NPL analyzed.

This subtask would be considered complete when a deposition process for an effective NPL that survives XCOM hybrid packaging was developed for testing.

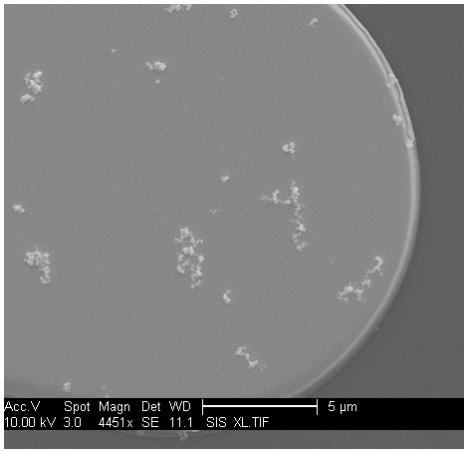

Figure 7: First NPL-covered XCOM relay contact prior to start of program.

Task 1, Subtask B – Modify NPL For Suitability

If modifications of liquid chemistry and/or nanoparticulates were to be required, then this subtask would be to modify them for enhanced survivability and performance. An ionic liquid corona, offers some advantages such as high fluidity, low melting temperature, high boiling temperature, thermal stability, and low vapor pressure. Other materials likely to be examined include bimetallic nanoparticles, which have exhibited excellent performance and durability in laboratory tests, including higher temperature (and likely hot-switch) survivability.

The synthesis of the initial gold NPL is summarized in the figure right. Chloroauric acid is dissolved and boiled. Sodium citrate tribasic dehydrate (SCTD) is added to produce Au nanoparticles with a SCTD corona. The solution is cooled and a molar excess of sodium 2-mercaptoethane (MES) is added, forming Au nanoparticles with a MES corona. Adogen is added as a positive ion source resulting in Au NPL with an ionic liquid corona. The Au nanoparticles are then collected, extracted into toluene, and purified by centrifugation and re-suspension in toluene.

This Subtask would be considered complete when an NPL that meets requirements were fully tested and transferred.

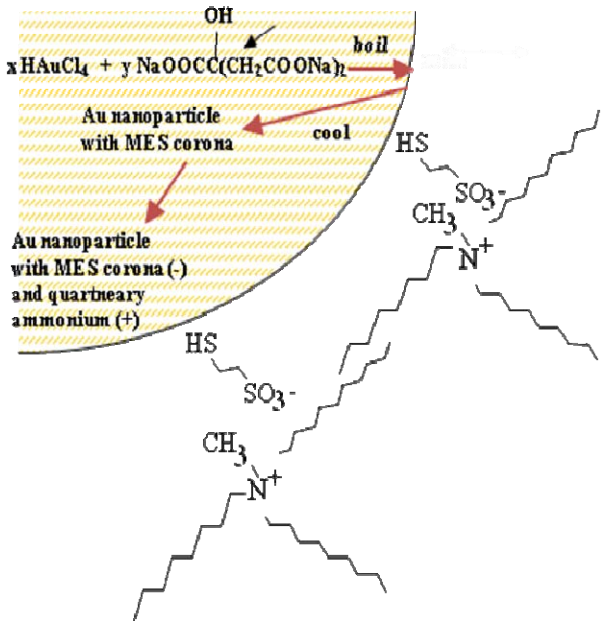

Figure 8: Synthesis chemistry for Au NPL

Task 1, Subtask C – Finalize Lubricant Material

This Subtask was an additional level of iteration in NPL development, and was segmented as a separate Subtask in order to more accurately represent milestones and dependencies. It was recognized that iterations of NPL materials and synthesis were required in the program for hybrid package and wafer package testing. This final material would then be used for the final stage of this program. It was assumed that some NPL material would ultimately provide some substantive benefit given the dramatic performance enhancements already tested in the laboratory and already shown to coat XCOM MEMS devices on the first crude attempts.

3.3.2. Task 2 – Implement NPL in MEMS Relays

The second task was to use the NPL in a standard RF MEMS switching circuit, a single-pole double-throw (SPDT) relay, so that the switching characteristics and power handling improvements could be accurately characterized using existing test sets, performance metrics, and test methods. This task included both hybrid and wafer-scale examination for both speed of process development and to attempt to meet the longer term tuning circuit product needs of the Defense radio community.

Task 2, Subtask A – Use NPL in Hybrid Packaged Relays

This Subtask was to deposit NPL into the hybrid packaging process used for the XCOM RF MEMS relay product. This would enable candidate NPL films to be examined for compatibility, and then tested in a semi-automated fashion for performance enhancement using existing product infrastructure. This allowed the largest risk of identifying a target NPL to iterate in the first year of the program. The XCOM RF MEMS device and package are shown below for size reference.

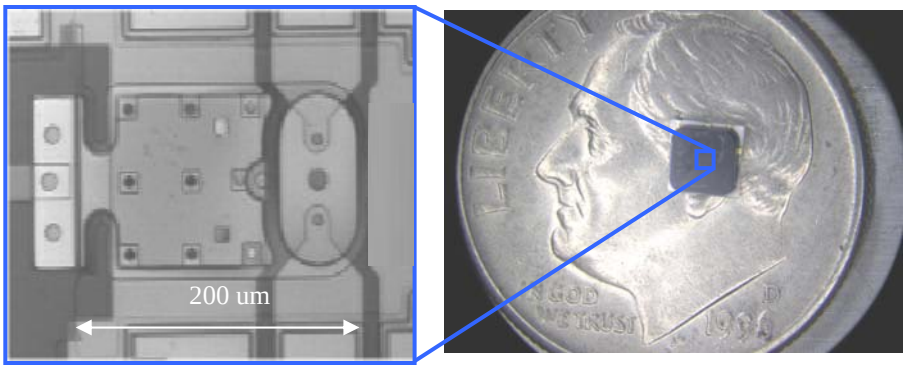

Figure 9: COTS hybrid packaged XCOM RF MEMS relay product.

The baseline process of assembly is provided below for reference. One aspect of this subtask is to modify the assembly process as little as possible in order to minimize the risk of adverse effects on the present COTS component performance. The first enhancement to be attempted would be to simply dip clean dies into NPL solution, let them dry, and perform die level tests to ascertain survival and unpackaged performance. If they survive, then the parts will be assembled and sealed as normal.

In the baseline process, the MEMS devices are released at the foundry (Innovative Micro Technology) on a wafer level using a proprietary combination of metal etches and rinses. They are then spin coated with a thick layer of soft-baked photoresist to protect the MEMS devices from a dicing operation. The wafer is then diced by a dicing supplier (American Precision Dicing) and returned to XCOM for post processing and assembly. The substrates, meanwhile, are manufactured, diced, and delivered from our ceramic package supplier (Vishay). The hybrid assembly steps are as follows:

1. Strip photoresist from die in heated n-methylpyrrolidone (NMP), do not let dry
2. Rinse in isopropyl alcohol, do not let dry
3. Rinse in AK-225 (California-approved final solvent for air drying) – die may be stored
4. Plasma clean the substrates and lids for 5 min. at 300W in oxygen
5. Stud bump substrates using a gold-silver alloy wire bonder – packages may be stored
6. Tack seal pre-form to lid – lid may be stored
7. Bake substrates and lids at 300 °C for 8 hours in a vacuum oven in low-pressure nitrogen
8. Bake die at 100 °C for 8 hours in a vacuum oven in low-pressure nitrogen
9. Flip chip die to substrate
10. Clip lid to package over die
11. Bake assembly in vacuum oven to seal ring profile in proprietary gas mixture

Task 2, Subtask B – Test Hybrid Packaged Relays

The primary purpose of this Subtask was to identify and quantify improvements in cold-switched, warm-switched, and hot-switched power handling and lifetime. This Subtask was to begin as soon as the first parts are available for testing after basic operational screening, and would not end until one or more likely NPL candidates were shown to be both survivable and effective. The basic operational screening determines that relays will open and close with a moderate resistance level (<10 Ohms) and capable of being examined with production test equipment and practices.

Once parts were determined to be operable, the RF lifetime tests to be performed would be within the range of power levels and operating conditions identified in the Table on pg. 6, which covers a wide range of parameters required by Government radio developers. Power levels available in commercial testing are 5 mW and 2 W, which are within the range of values of interest. Testing needed be performed on at least 8 devices in accordance with accelerated testing practices. For each test, a subset of failed and operable devices would undergo destructive microscopy analysis. Once candidates have shown warm-switch power handling improvements, then extended life testing on cold switching and repeatability would commence.

Task 2, Subtask C – Examine NPL Deposition for Wafer-Scale Packaged Relays

In this Subtask, NPL candidates would be applied in a deposition process compatible with IMT's release and cleaning process as part of the Xipe-Totec wafer-scale packaging used for XCOM and Harris tuning and filter circuits. This Subtask would begin when the candidate NPL materials and processes were vetted through the hybrid packaging process with appropriate modifications already made.

There were two risks in this Subtask associated with the two technical thrusts required for these components. The first risk was that no NPL candidate would found that can be easily transferred, and that would be determined during this Subtask effort. The second risk was that the wafer-scale process would have difficulties during the program, independent of the progress of the NPL type, manufacture, and deposition process.

Task 2, Subtask D – Test Wafer-Scale Packaged Relays

This Subtask is to test wafer-scale packaged components in the same manner as the hybrid versions using test equipment that was not presently available as of the time of the proposal. This Subtask would begin once parts were available, and would end after parts were tested.

In addition, at this higher level of integration it was (and still remains) of interest to perform radiation testing using the harnesses and methodologies already having been used to test RF MEMS. This would include realistic gamma doses, neutron doses, and heavy high-energy particles. Initial testing already reports good survivability for IMT MEMS films essentially identical to those used in XCOM devices.

3.3.3. Task 3 – Demonstrate Improved Efficiency

Amplifiers are the largest consumers of radio power, and typically operate below 20% and get worse with changing antenna conditions (terrain, position, etc.), changing power needs (edge of range, temperature, ageing), and frequency. Dynamic tuning can compensate for all of these effects, recovering and maximizing efficiency at or above 50% over all conditions, resulting in improved battery life and data link quality. This task is to design a power amplifier and demonstrate improved efficiency with MEMS-switched high-Q capacitors.

Task 3, Subtask A – Design Tuning Circuit

The first subtask was to design a tuning circuit that works with a broadband power amplifier in a relevant tactical radio frequency range. A suitable power transistor requires input and output matching circuits, as well as a biasing circuit. A common matching circuit for the output would use several fixed inductors with switchable capacitors, keeping Q>100 at 1 GHz. These kinds of multi-state capacitor specifications are achievable only with the "switched bank" architecture. This Subtask was to begin when the team developed a moderately high level of confidence in candidate NPL lubricants, and after initial tests with NPL-enhanced hybrid packaged MEMS devices. This Subtask would end when an amplifier and tuning circuit were designed.

Task 3, Subtask B – Assemble Amplifier Circuit

Once NPL-enhanced RF MEMS tuning circuits were available, the team would assemble a laboratory brassboard demonstration of a multi-waveform radio amplifier. The board material would be designed to accommodate the COTS broadband amplifier, integrated passive and chip inductors, and MEMS tuning circuit. The components would be assembled and functionally tested. This Subtask would have begun when the first packaged NPL-enhanced relays were fabricated and operationally tested. This Subtask would have ended when the amplifier circuit was complete and ready for testing.

Task 3, Subtask C – Test Amplifier Circuit

This Subtask was to test the tunable amplifier circuit for a broad range of RF performance, efficiency, heat generation, power output, input bias, temperature, instantaneous bandwidth, center frequency, and de-tuning operating conditions. This Subtask would begin when the amplifier circuit is complete and ready for testing. This Subtask would end when it had been fully tested for RF and thermal performance.

Operating conditions of interest include output impedance varying between 25 and 150 Ohms, amplifier bias voltage varying from 70-120%, temperature from –55 to +85C, and should consider a significant subset of JTRS and future radio bands selected from 30-88 MHz SINCGARS all the way through 6 GHz IMS bands. For testing, a thermocouple harness or spot measurement system could verify thermal performance of the amplifier, with heat generation, power input, power output, and efficiency directly measured.

4. Results and Discussions

Nanoparticle liquids (NPLs) are a new class of materials comprised of nanoparticles with an inorganic nano-sized core and ionic liquid corona.[1,2] Early experiments determined that they may be suitable for lubricating metallic RF MEMS switching devices using a nanoparticle core of metal to facilitate electrical conduction. Laboratory experiments with experimentally modeled switch surfaces showed that NPLs can address the problems of erosion, shorting, adhesion, and other failure mechanisms.[3] NPLs could represent a paradigm shift for surface contacts due to nanotexturing, high surface slope, liquidity/reflow, and multiple delocalized contact spots.

Three tasks were conceived to develop NPL technologies and implement them into RF MEMS switching devices. First, candidate NPL materials would be examined for manufacturability and potential usage in switching. Second, the NPL would be transitioned to the XCOM RF MEMS relays and tested. Third, a demonstration circuit would be developed to demonstrate the potential system value of these technologies. The results of these three tasks follow.

4.1. Task 1 – Develop Nanoparticle Lubricant

To begin the program, a UDRI synthetic chemist reviewed procedures in place for the synthesis of the original gold NPL. Background research for the ordering of chemical stock was conducted, and a number of chemicals required for synthesis were ordered in preparation for the first chemical reaction. UDRI also ordered and received the necessary labware for NPL synthesis. A hood in AFRL/RXBN was secured, cleaned, and set up to carry out the chemical reactions. The required solvents were ordered and secured for synthesis. The base bath for cleaning glassware was set-up in preparation for use.

4.1.1. Task 1, Subtask A – Develop NPL Deposition Process

In this first Subtask, we were to develop methods to apply existing NPLs to XCOM MEMS devices at some point in the MEMS die cleaning, post-processing, and/or packaging steps. NPLs with a 20 nm Au core and a mercaptoethane sulfonate (MES) and quaternary ammonium (adogen) corona were chosen as the initial lubricant for study. The ionic liquid corona offers enhanced electrical conduction, thermal stability, and excellent fluidity of the NPL due to the branched and long hydrocarbon chains of the quaternary ammonium.[4]

Prior to the start of the program, NPLs had initially been applied to comparatively featureless surfaces using both dip-coating and spin-coating techniques. In both cases, the NPLs were visible on the surface without aggregation ("clumping") and were relatively stable in terms of remaining on the surface throughout testing. Application of NPLs to surface-micromachined MEMS surfaces, however, was a much greater challenge, so optimization and technical assessment of coating processes is an important part of this program. XCOM uses a NMP $\rightarrow$ isopropyl alcohol $\rightarrow$ AK-225 die cleaning process. The starting plan was to apply the lubricant in an additional AK-225/NP solution dip coating step. Studies using various concentrations of nanoparticles were needed to optimize coverage as determined with a scanning electron microscope (SEM). This is to give us ball park ideas of coverage and film quality.
Thermal stability of the NPL has always been of particular interest due to elevated temperatures experienced during any higher-quality hermetic packaging processes. In the XCOM hybrid

packaging process, the NPL must withstand 240 °C for 30 s under nitrogen with a low-moisture reducing gas mixture. Thus, thermal stability experiments using thermal gravimetric analysis (TGA) and/or differential scanning calorimetry (DSC) are pertinent to the survivability of the lubricant in the manufacturing process.

A high purity NPL material will enhance the chance of success, and will require an emphasis on procedures that lead to a cleaner product and quantitative analysis. High purity NPL has minimal excess corona material, i.e., corona material not attached to a NP. Excess material can degrade under electrical and thermal stress that can lead to film growth and performance degradation, which can detract from the benefits provided from the NPL. Thermal degradation experiments using TGA can provide information on the thermal stability of the NPLs.

Synthesis of sufficient material for process development and characterization is important in transferring NPL technology from the laboratory to MEMS process compatible production. To support the XCOM hybrid packaging process, 200 – 500 mL of quality material at various concentrations is required and thus is the desired product of the synthesis efforts. Fortunately, the liquid-based synthesis is also compatible with liquid based processing of MEMS switches. The initial synthesis of NPLs was performed using the following procedure:

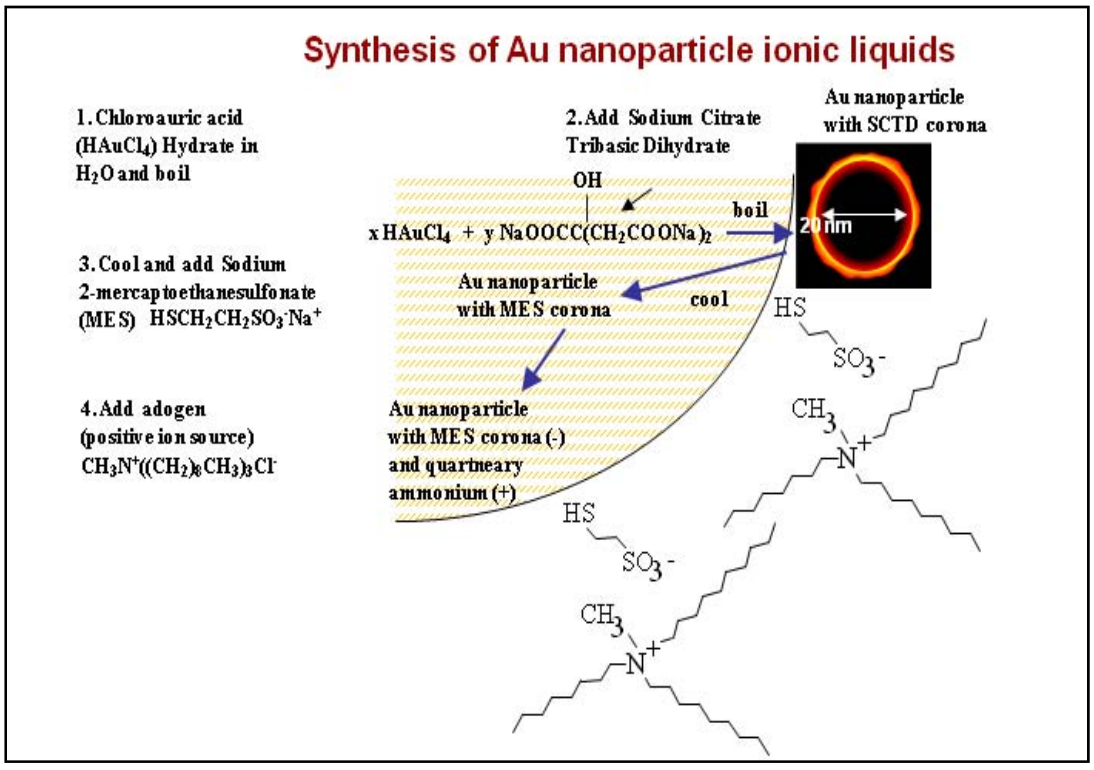

Figure 10: Synthesis procedure for Au NPLs (after Fig. 8)

Gold Nanoparticle Ionic Liquid Synthesis Procedure

1. Make 20 nm citrate NP:

Clean the beaker in base bath for 2+ hours. Rinse with DI water. Clean beaker with aqua regia. Rinse 3x with milli-q H20.

2. Make gold solution

Add 68 mg HAuCl4 to 6.8 mL milli-q water.

3. Make citrate solution:

Add 400 mg sodium citrate to 40 mL milli-q water.
Add ~750 mL milli-q water and gold solution to cleaned beaker and bring to reflux while stirring vigorously. Add citrate solution and stir until it turns ruby red. Let cool.

4. Diafiltration :

Take total volume down to 10-30 mL and transfer to a 50 mL centrifuge tube.
To determine concentration of gold by Ultraviolet-Visible Spectroscopy (UV/VIS): Dilute the product to 50 mL and dilute that by 8 times:
Transfer 4 mL gold-citrate NP into cuvette 1
Transfer 2 mL of cuvette 1 to cuvette 2 then add 2 mL additional DDW to give 4 mL
Repeat with cuvettes 3 and 4 to give a total dilution of 8 times—it should now be dilute enough to give OD=1 by UV/VIS (approximately)
UV/VIS: run a blank of DDW; then run the sample--look for a peak at 520-522nm and record the absorbance (should be close to 1). Use this in Beer's law to give the volume of water needed to maintain a gold concentration of OD=1 (should be close to 700 mL).
Determine the exact concentration of gold in solution in mols. The ratio of gold to MES = 1. Now the amount of MES can be determined.

5. 2. MES (ligand) addition:

Add MES to gold/citrate solution with stirring
Stir about 2 hrs—color will change to a bluer purple
Repeat diafiltration and UV/VIS as above to give amount of Adogen to add.
The ratio of MES to Adogen should be 0.1

6. Adogen 464 (surfactant) addition:

The gold/MES sample can be left in water.
Adogen should be added to toluene (or other water insoluble solvent) to give a solution.
Add both solutions to a beaker with stirring and stir several hours to overnight.
Transfer to separatory funnel and remove the water (can be dried over molecular sieves).
Filter through Omnipore PTFE 0.1 μm membrane.

Initial synthesis attempts were not particularly successful, and a significant amount of creative physical chemistry work was performed. For example, in the first attempt to synthesize NPLs using the stated procedure, the gold-citrate solution was synthesized and concentrated using a centrifuge. A hard pellet was formed that could not be recovered.

On the second synthesis attempt, the final product was made but subsequently lost when attempting to take it up in isopropanol. The reaction went as expected until the adogen was added to the Gold/MES solution in water. The solution turned a murky violet color indicating poor solubility. The solution was then filtered using a peristaltic pump and UV/VIS was run on the sample. It gave an OD=1 at 538 nm (should give at about 520 nm). This indicated the presence of larger particles. It was filtered through a 1 μm membrane and centrifuged 30 min at 8500 rcf to remove the supernatant. Isopropanol was then added (50 mL to each centrifuge tube) and sonicated to break up the particles. It did not form a hard pellet as in the case of gold/citrate, but gave a cloudy indigo suspension that slowly settled out of solution. Next, the suspension was transferred to a separatory funnel, more isopropanol was added and residual water taken off (5-10 mL). Then the solution was filtered through the 1 μm membrane, but the solids stayed on the membrane. This is clear evidence that isopropanol is not an acceptable solvent for this product. Attempts to recover the product by soaking the membrane in toluene were unsuccessful.

The next attempt to make the gold citrate ran into problems with the gold plating out on the tubing while using the peristaltic pump. It was found that filtering the solution through a fritted funnel took care of that problem. The next approach was to complete the reaction in water to the gold/MES stage. At that point an adogen 464/toluene solution was made and added to the aqueous solution. The gold/MES should migrate from the water to the toluene and react with the adogen there. The toluene can then be separated from the water and the concentration of gold determined by UV/VIS.

Some other problems arose during synthesis efforts. One problem was associated with the weighing out of chloroauric acid. It gained weight on the balance and started to bubble on the stainless steel spatula (giving off HCl). It was suspected that the problems were due to a higher humidity in the lab due to the arrival of warmer weather. It was subsequently weighed out in a dry glove box with no further problems. Some issues related to solubility also arose. Au-MES is not soluble in toluene, and adogen is not soluble in water, although adogen is soluble in toluene. The purpose of using adogen is that it serves not only as a surfactant but also as a phase transfer agent to move the Au-MES into the toluene or other organic solvent. One method of overcoming this difficulty is to use excess adogen dissolved in toluene and add that to the Au-MES aqueous solution with vigorous stirring. The downside of this is that it is difficult to remove the excess adogen and the shelf life of the solution is limited due to the gold nanoparticles separating out.

What had originally been perceived to be a straightforward enhancement of the first synthesis operation already used by UDRI ultimately turned into many months of development work in order to obtain initial samples. The end result is that the deposition techniques were delayed until after the second subtask, as considerable NPL process modification had to be undertaken before deposition could proceed. The solution for the NPL had to be complementary to XCOM die-level and wafer-level post-processing, so the NPL had to be modified.

4.1.2. Task 1, Subtask B – Modify NPL For Suitability

With the production delay, continued work on NPL modification and manufacture continued in earnest. The primary goal was to deliver a sufficient quantity of NPL with an appropriate solution for deposition that was compatible with RF MEMS devices and packaging. Earlier tests resulted in mixtures that settled out of solution, forming aggregates that prevented the proper dispersion of particles. In addition, deposition with water rinse or dilution was confounded with the presence of salts out of solution, later determined to have been caused by laboratory equipment at XCOM. The end result was an inability to deposit NPL with the original solution.

An interesting experiment was done using the surfactant TOAB: $(C_8)_4NBr$. TOAB has a structure similar to adogen, $(C_{8\text{-}10})_3CH_3NCl$, and should display similar solubility. To a Au-MES solution in water, three different concentrations of TOAB dissolved in toluene were added with stirring: 3:1, 1:1, and 1:3 Au-MES: TOAB. All went into the toluene after 5-10 min. The water was removed using a separatory funnel and the samples were left to stand for a month. The 3:1 did not stay in solution at all. The 1:1 stayed in solution longer but the gold started plating out on the sides of the flask after a few days. The 1:3 stayed in solution the longest but has plated out some also. This would indicate the importance of molar concentration. This led to a comparison of different methods of making the Au-MES-adogen. Table 1 compares three methods that have been used in AFRL/RXB. The main differences lie in the amount of MES and adogen used.

Table 4: Three Synthesis Methods for Au-MES/Adogen.

	Method 1	Method 2 - MEMS, Vol.17, No.3, June 2008	Method 3 - SMALL, 2007,3, No.11, 1957-1963
Chloroauric Acid	0.68 g / 800 mL 2.5mM	0.68 g / 800 mL 2.5mM	0.68 g / 800 mL 2.5mM
Sodium citrate tribasic	5% = 400mg	Stoichiometric amt. 2.5mM = 588mg	Stoichiometric amt. 2.5mM = 588mg
MES	1:1 MES:Au 3.25 mg 1*	fivefold equivalent 12.5mM, 36.7g	fivefold equivalent 12.5mM, 36.7g
Adogen 464 (insol. in water)	0.1:1 Adogen:MES 0.886 μL	fivefold equivalent 12.5mM, 3.56 ml	twofold equivalent 5.0mM, 1.42 ml 2*

1* Outer surface of NP MES will bond with every 3rd or 4th outer molecule (dep. on number)
2* Purification: Centrifuge and re-suspend in water and ethanol (5 times) Insol. in water; sol. in toluene (ruby colored) Au content 10-80%, depends on purity, excess mass due to adogen

A solubility study was performed in which we placed Au-MES aqueous solution in test tubes, added organic solvents, and shook to mix. We added: toluene and toluene with adogen; AK-225 and AK-225 with adogen; and ethyl acetate and ethyl acetate/acetonitrile. In all cases the Au-MES stayed in the aqueous layer as noted by the red color. It was decided to do a study of solubility based on polarity as determined by Hansen Solubility Parameters and water solubility. The results shown in Table 2 were obtained using Molecular Modeling Pro Plus, version 6.2.2. The structure of interest is drawn and the computer program displays the results based on various calculations and literature data. The results indicate that as the number and length of alkane chains increase, the polarity and solubility decrease.

The solvents chosen for this study range from a polarity of 0 for AK-225 to 16 for water. By choosing a surfactant with polarity close to the polarity of a solvent, the likelihood of solubility increases. Effects of surfactant concentration and polarity were used to facilitate obtaining the final product in organic solvent.

Table 5: Hansen solubility study.

mono, di, tri, and tetra-substituted dodecyl ammonium salts						
Chemical	Formula	m.p. (^{o}C)	Polarity	Hydrogen Bonding	Solubility Parameter	Water Solubility (g/L)
Dodecyltrimethyl ammonium bromide	$[CH_3(CH_2)_{11}]N(CH_3)_3Br$	246	2.64114	4.06289	16.5775	$5.67x10^{-3}$
Didodecyltdimethyl ammonium bromide	$[CH_3(CH_2)_{11}]_2N(CH_3)_2Br$	157-162	1.66389	3.2248	16.835	$1.91x10^{-8}$
Tridodecylmethyl ammonium chloride	$[CH_3(CH_2)_{11}]_3N(CH_3)Cl$	110-112	1.21451	2.75512	16.9778	$5.26x10^{-14}$
Tetradodecyl ammonium bromide	$[CH_3(CH_2)_{10}CH_2]_4N(Br)$	89-90	0.956251	2.4447	17.0666	$1.31x10^{-19}$
Solvents						
Solvent	Formula	b.p. (^{o}C)	Polarity	Hydrogen Bonding	Solubility Parameter	Water Solubility (g/L)
AK-225	Dichloropentafluoro propane	54	0	0	7.59298	$8.65x10^{-3}$
Toluene	$C_6H_5CH_3$	111	0.749	1.98	18.125	0.422
Isopropanol	$(CH_3)_2CHOH$	82	6.8703	17.4066	24.5348	137.54
Water	H_2O	100	16	42.3	47.8	1180
Ligands						
MES	$HSCH_2CH_2SO_3Na$	n/a	21.1973	12.494	31.7764	333.51
Additional Surfactants						
Chemical	Formula	m.p. (^{o}C)	Polarity	Hydrogen Bonding	Solubility Parameter	Water Solubility (g/L)
Adogen 464 Methyltrialkyl(C8-C10) ammonium chloride	$CH_3[(CH2)_{8\text{-}10}]_3N(Cl)$	semi-solid	1.5597	3.1222	16.8749	$1.88x10^{-9}$
TOAB Tetraoctylammonium bromide	$[CH_3(CH_2)_7]_4N(Br)$	95-98	1.38552	2.9427	16.9346	$1.75x10^{-12}$
Tetrahexadecyl ammonium bromide	$[CH_3(CH_2)_{15}]_4N(Br)$	97-100	0.73006	2.13609	17.1414	$9.37x10^{-30}$
Tetraoctadecyl ammonium bromide	$[CH_3(CH_2)_{17}]_4N(Br)$	103-105	0.65284	2.01998	17.1678	$6.16x10^{-33}$

Solubility and compatibility issues were found to be critical in NPL synthesis. Researching these areas led to new ways to solve these problems.

Concentration of the Ligand: One of the things we became aware of is that MES (the ligand we used) tends to equilibrate in water. We had been using a 1:1 ratio of MES to gold (standard procedure). It was decided to go to a 5:1 ratio of MES to gold, eliminate washing the MES-Au solution with water as a purification step, and reduce the volume of water from 800 mLs to 80 mLs before introducing the surfactant. This was to ensure that a sufficient number of sulfur bonds have attached to the gold NP.

Ligand-Surfactant Reaction: A new approach for attaching the surfactant to the MES was needed. Because the organic solvents (toluene and AK-225) are so non-polar, it was necessary to dissolve the surfactant in the organic solvent (100 mLs) then add the MES-Au (in 10 mLs of water) with vigorous stirring. The surfactant is in a 1 molar ratio to the MES and the gold concentration remained at about OD=1. Once the MES-Au moved into the organic solvent by reacting with the surfactant, the next step was to clean up the product.

Purification: The diafiltration apparatus could not be used to filter out the smaller free-floating MES-surfactant molecules because toluene and AK-225 can damage the plastic in the filter and also the tubing. It was decided to centrifuge the product with the idea that the free-floating MES-surfactant molecules (unbound to the gold NPs) could be removed by pipette, more solvent added and the process repeated to remove as much unbound material as possible. Centrifuge tubes made of Teflon were ordered and used for this purpose.

Experiments: The issue of the ligand concentration is a very important concept to investigate. It was reasoned that by reducing the volume of water of the gold-citrate solution prior adding the MES there would be less tendency of the MES to equilibrate in the water and more sulfur bonds could form. The gold-citrate was made as usual then reduced in volume via the diafiltration pump, washed with 300 mL DDW, then taken up in 80 mL DDW. MES was added (5:1 MES:Au) and stirred for 5 hrs. Upon filtering through a 0.1 μm membrane the gold filtered out.

To address the problem of attaching the surfactant to the MES it was decided to dissolve the surfactant in an organic solvent before adding to the gold-MES. An experiment was set up in which four surfactants were dissolved in two solvents: toluene and AK-225. The four surfactants are Adogen 464 (C8-C10), TOAB (tetraoctylammonium bromide) (C12), tetrahexadecylammonium bromide (C16), and tetraoctadecylammonium bromide (C18).

Each of the eight reactions contains 100 mL gold-MES solution in water and an equal amount of organic solvent containing the surfactant. Each was stirred 2-4 min. and allowed to stand 2 weeks. The goal was to obtain a good product in AK-225 since it is used as the final rinse in the XCOM process. Toluene was also be used because it has very low polarity (0.75) comparable to AK-225 (0). This will contribute to the reliability of the results to have a comparison of the two solvents, and procedures using toluene in gold NP synthesis are available in the literature. The eight reactions (4 in toluene and 4 in AK-225) were to be observed for completeness of the transfer from water to the organic solvent and the shelf life of the product (noting any precipitation or plating out on the sides of the beaker). Table 3 shows the results of the experiments. The desired NPL product did not form in the organic solvent in any of the cases. This was disappointing, but was also a good indicator that a different approach was needed to form the desired NPL product in an organic solvent.

Table 6: Results of surfactant solubility studies in toluene and AK-225.

Toluene		AK-225	
Adogen			
Toluene layer (top)	pale pink	Water layer (top)	colorless-gold film
Interface	no color or solids	Interface	blue solids
Water layer (bottom)	dark red-purple	AK-225 layer (bottom)	colorless
TOAB			
Toluene layer (top)	colorless	Water layer (top)	ruby red-gold film
Interface	blue solids	Interface	blue solids
Water layer (bottom)	pale purple	AK-225 layer (bottom)	colorless
C16			
Toluene layer (top)	Colorless - gold on glass	Water layer (top)	white ppt, gold film
Interface	no color or solids	Interface	blue solids
Water layer (bottom)	pale pink	AK-225 layer (bottom)	colorless
C18			
Toluene layer (top)	colorless	Water layer (top)	ruby red
Interface	gold sheen	Interface	white ppt.
Water layer (bottom)	colorless-dark blue solid	AK-225 layer (bottom)	colorless

4.1.3. Task 1, Subtask C – Finalize Lubricant Material

A modified synthesis approach allowed the successful transfer of the NPL from water into toluene. This was a very significant step as this gave us a NPL product in a suitable solution to apply to the XCOM device. This method used a fivefold excess of MES to auric acid and a tenfold excess of Adogen to auric acid. The synthesis of the gold citrate followed by MES exchange followed the same general procedure as previous efforts with a few minor modifications. For example, before adding the sodium citrate, the water was brought to a full rolling boil which helps to avoid aggregation. Also, a new bottle of auric acid was used and stored in a desiccator in the glove box. Adogen was added as a mixture by stirring it into a small amount of water with a spatula while adding to the rapidly stirring Au-MES solution.

A new approach to isolating and cleaning the product was undertaken and resulted in a successful transfer into toluene. The product was transferred to Teflon centrifuge tubes and centrifuged for 45 min. at 8500 rcf forming a pellet of NPL. Most of the water (containing excess MES and adogen) was removed by pipette and the rest was combined into 4 centrifuge tubes (about 20 mLs each) and toluene was added (about 25 mLs). This was centrifuged for 15 min at 8500 rcf and again the water was removed by pipette. Upon shaking, the product dissolved in toluene to give a ruby red solution. The toluene extracts were collected and taken to dryness under nitrogen flow. It readily re-dissolves in toluene as a ruby red colloid but precipitates out in AK-225. The lack of solubility in AK-225 does not allow applying the NPL to XCOM die using an additional AK-225/NPL step added to the end of their die cleaning process.

Additional Au-MES-Adogen synthesis experiments were conducted to confirm the repeatability of the synthesis process. Confirmation of the successful synthesis in independent runs is a crucial step in the program as it ensures that sufficient material is available for MEMS switch lubrication experiments and physical and chemical characterization. It also provides the foundation for altering NPL structure for enhanced performance as a MEMS switch lubricant, if such modifications are needed. Table 7 summarizes synthesis parameters and UV-VIS transmission results for four successful synthesis runs.

Table 7: Au-MES-Adogen reactions.

Gold and Citrate additions					
	400 ml water		UV-VIS of Au-Citrate (in water)		
notebook no.	HAuCl4 (mg)	NaCitrate (mg)	wavelength (nm)	absorbance	mLs needed to give OD=1
	(0.25mM in 400mL)				
NP-SS-11	36 (0.26 mM)	200	520	1.079	440
NP-SS-14	34 (0.25 mM)	200	521	1.316	520
NP-SS-20	35 (0.26 mM)	200	N. A.	N. A.	N. A.
NP-SS-24	35 (0.26 mM)	200	521	2.297	920

MES and Adogen additions					
			UV-VIS of Au-MES-Adogen (in toluene)		
notebook no.	MES (mg) 5:1 MES:Au	Adogen (mg) 10:1 Adogen:Au	wavelength (nm)	absorbance	mLs to give OD=1
	(0.125mM in 400mL)	(2.50mM in 400mL)			
NP-SS-11	8.3 (0.112mM)	400 (2.29mM)	529	0.2366	95
NP-SS-14	10.1 (0.115mM)	400 (1.94mM)	530	0.2558	102
NP-SS-20	10.1 (0.114mM)	400 (1.92mM)	530	1.4530	580
NP-SS-24	18.0 (0.116mM)	94 (0.25mM)	530	0.9157	366

The formation of the gold-citrate solution continued to be a challenge, as it was very sensitive to conditions. The extent of cleanliness required in this step was illustrated by NP-SS-20 which had the best yield as determined by UV-VIS absorbance in toluene (1.4530). This reaction followed four failed reactions in which the gold precipitated out. To correct this, the beaker and stir bar were submerged in a base bath for several hours and rinsed with water, then a freshly made solution of aqua regia was added to the beaker, stirred for 20 minutes and rinsed with copious amounts of distilled water and deionized water. Also, the tubing and reservoir on the diafiltration pump were changed. The objective was to make sure there were no deposits on any surface that might serve as a location for the gold to precipitate out on. Smooth glass coated stir bars were purchased along with a beaker heating mantle to keep the temperature even throughout the reaction. This is consistent with reports in the literature that reported that particular attention to the cleanliness of glassware is important to successfully synthesize gold NPs.[5] The figures below illustrate various aspects of the NPL synthesis process.

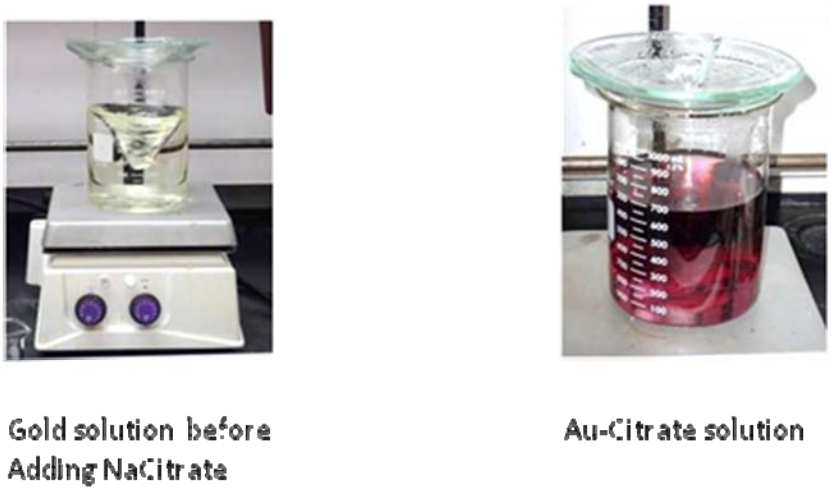

Figure 11: Photographs of nanoparticle solution during Au-citrate synthesis

Figure 12: Schematic of diafiltration pump, Au-citrate purification, and UV-VIS Specimens.

The sample NP-SS-14 was analyzed using an FEI Titan transmission electron microscope (TEM) at 300 kV accelerating voltage and showed excellent spherical shape, size dispersion, and separation. Figure 13 shows the effect of the NPL corona on controlled particle interactions, where no particle fusing occurs due to mediation of strong metallic bonding forces. The corona can be seen directly in the high resolution TEM image in Figure 14. Thus, TEM confirms the successful synthesis of NPL by the presence of the ionic liquid corona and the liquid-like interaction between NPL particles.

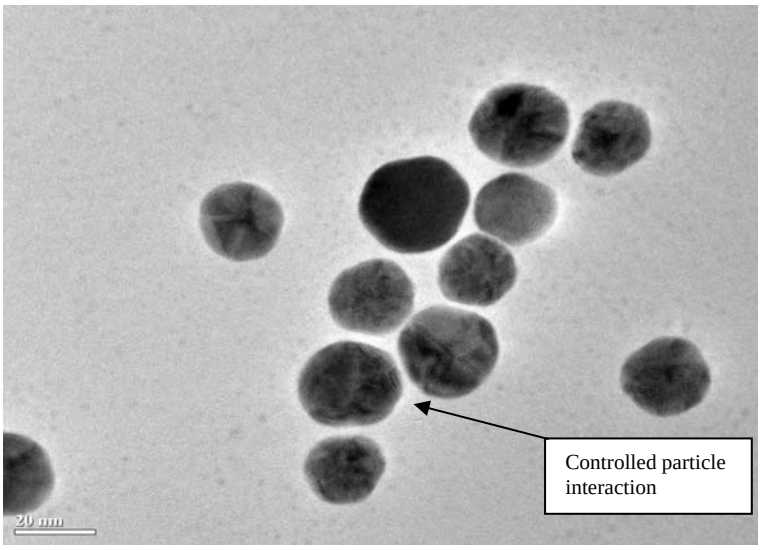

Figure 13: TEM Images of NPL at 115,000 X

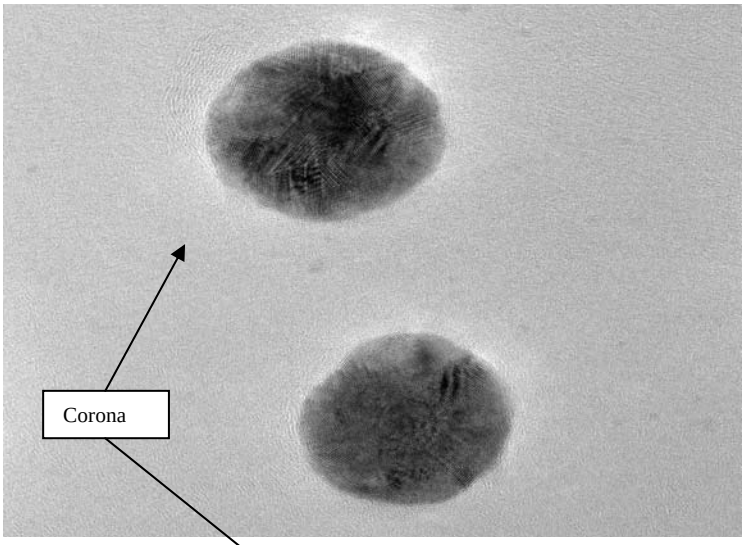

Figure 14: TEM Images of NPL at 300,000 X

One of these reactions was prepared in three different concentrations of NPL in toluene. These were sent to XCOM along with a pure toluene specimen for application to RF MEMS relays. Reactions were run in water, then concentrated by centrifugation, and finally taken up in toluene with volume adjusted to 50 mLs. Two mLs from the 50 mL solution was diluted with two mLs of toluene and absorbance (A) was measured by UV-VIS at 1.453. In spectroscopy, the

absorbance is called optical density (OD) and is defined as $A = \log_{10}(I_0/I)$, where I is the intensity of light at a specified wavelength λ that has passed through a sample, and I_0 is the intensity of the light before it enters the sample. Concentration is determined from Beers Law:

$$A = ebc, \quad (1)$$

where b = path length = 1 cm (1 cm cuvette), e = 3900 L/mol cm (the extinction coefficient for gold), and c is the concentration in mol/L. As an example, if the absorbance measured by UV-VIS is 1.0, then c = A/eb = 1.0 / [(1 cm)*(3900 L/mol cm)] = 2.56×10^{-3} mol/L. The four samples sent to XCOM had ODs of: 0 (pure toluene); 0.027; 0.29; and 2.906.

Thermal stability of the lubricant film is important for survivability during both the packaging process (up to 240 °C) and during operation. Au-MES-Adogen NPL thermal stability was investigated by TGA. A reaction (in toluene) was taken to dryness under nitrogen and provided enough dry product for one scan. The temperature profile was isothermal at 40 °C for 20 minutes followed by a 10 °C/min ramp rate to a temperature of 850 °C, with TGA results below.

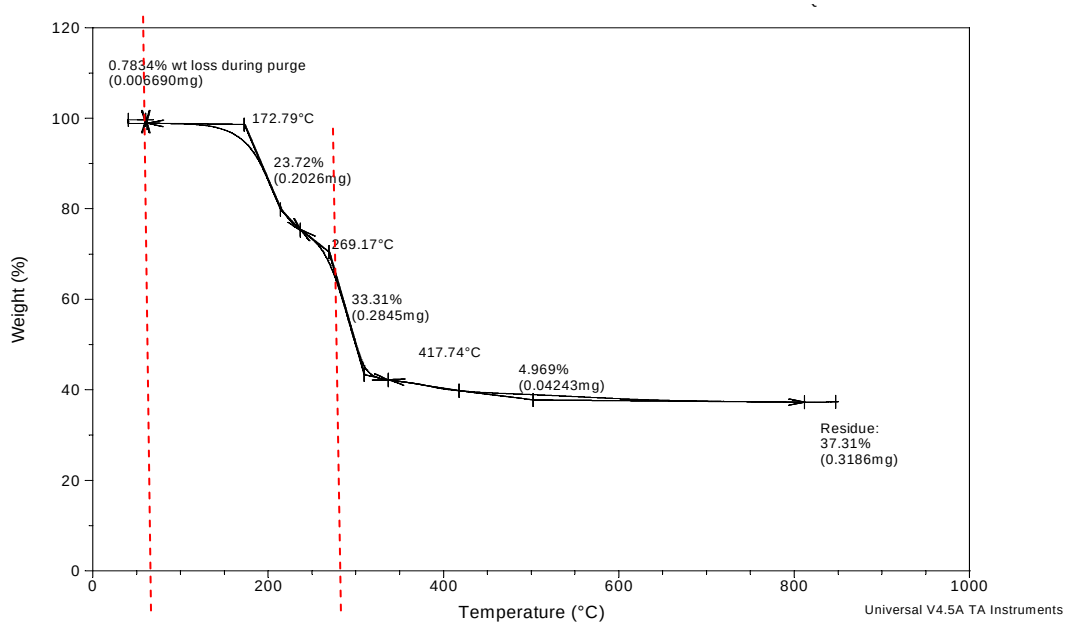

Figure 15: TGA Data of Au-MES-Adogen 464 NPL.

A previous study reports the onset of thermal decomposition of Au-MES at 260 °C.[6] This is most likely the origin of the second large mass loss at about 260 °C. The implication could be that the first mass loss is due to thermal decomposition of the Adogen, although this has not been proven. The other important point to note is that the sample is exposed to a much more aggressive condition as far as the time and temperature compared to the packaging process.

4.2. Task 2 – Implement NPL in MEMS Relays

The second task is to deposit the NPL material into the MEMS relays in a manner that is compatible with the hybrid and wafer-scale packaging techniques used by XCOM. Unfortunately, the manufacture of material took approximately a year, traversing through many stages of NPL modification and process development before stable material could be produced and delivered for deposition process development. Once this was accomplished, however, research into deposition, solvent analysis, and device testing was able to proceed at a rapid and effective pace.

4.2.1. Task 2, Subtask A – Use NPL in Hybrid Packaged Relays

The first substantive subtask was to add the material to bare die and then package them in the hybrid devices similar to the COTS relays already in production and qualification. For the first tests, the NPL was deposited as an additional droplet deposition, then dipping step performed after the normal die stripping and cleaning process. The initial plan was to start with pure toluene (OD = 0) as a control and gradually work their way up in concentration looking for changes in relay performance as the lubricant was applied.

The initial plan encountered problems immediately, as a solid bridging problem was identified during control experiments with pure toluene. A four actuator dual single pole double throw die was dipped in toluene and then dried on a hot plate for ten minutes at 240 °C. It was observed that three of the four actuators had failed and were stuck down in the closed position, and one actuator had failed in the open position. All electrical and RF testing resulted in no movement or electrical contact of any kind. The actuator beams were removed with tape and optical micrographs were taken of the beam underside and die topside at the contact region. Figure 16 below shows dark spotting evidence of solid bridging on the die topside and beam underside.

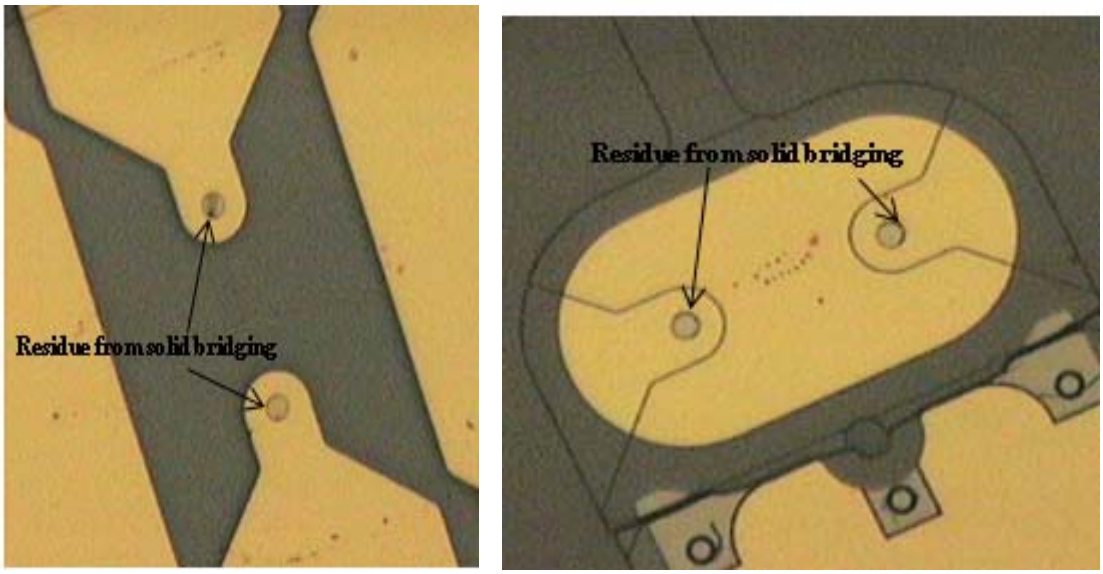

Figure 16: Micrograph of die topside and beam underside showing residue from solid bridging.

It was determined that the drying of toluene resulted in a sticky residue to remain at the points of contact and surface-tension based final connection and drying point. This point, of course, was the contacts themselves, so the drying of toluene necessarily meant that NPL as well as solvent residue remained to coat the contacts (and adhere them together in most cases) in a comparatively thick film that could not be broken by the actuator or signal loads.

Due to the toluene-based solid bridging problem, a solvent other than toluene was explored for coating the Au-MES-adogen material. A different surfactant (to replace adogen) might have been found that is compatible with an alternate solvent. It may even have been that toluene dissolves other residue present on the die after etch and die cleaning. Thus, getting the NPL into an alternate solvent that does not dissolve and redeposit residue on the contacts is a second type of approach to overcome the solid bridging problem.

A solubility study was conducted to find a suitable solvent to replace toluene. A new batch of Au-MES-Adogen was synthesized in water by the usual method, centrifuged, and the product transferred from the water to the toluene. The toluene was then evaporated to dryness. Each solvent (approx. 10 mL) was added to a dried sample, shaken, and allowed to stand. If the product started to precipitate out of solution within a few hours it was left to stand 24 hrs before categorizing as slightly soluble or very slightly soluble. If the product didn't precipitate out at all, it was left to stand for 3 days before categorizing as soluble.

The most promising candidate, p-xylene, has the same structure as toluene with one more methyl group. Getting the product into a solvent from the dry state is more difficult than transferring it from water to that solvent. This is evidenced by the inability of water to dissolve the product from the dry state even though the product had originally been a solution in water.

TOAB is less polar than Adogen, and thus may be more compatible with less polar solvents. A previously synthesized reaction of Au-MES-TOAB, which would not transfer into toluene from water, was evaporated to dryness. It would not go back into water, was insoluble in chloroform, and had unpredictable results in NMP. By adding about 5 mls of ethanol, then adding about 20 mLs of 2:3 isopropanol: hexane mixture, a colorless solution was obtained. After 2 weeks a dark blue precipitate had formed.

A second batch of Au-MES-TOAB was synthesized. Efforts to dissolve TOAB before adding it to the Au-MES solution resulted in the observation that TOAB was insoluble in toluene, acetone, water, chloroform, isopropanol, chlorobenzene, benzene and p-xylene. These solvents were chosen based on their polarity. However, TOAB did dissolve in hot ethanol and was added to the reaction with vigorous stirring. The clear red solution became milky red. Upon vacuum filtration, most of the solids filtered out to give a clear, colorless solution (most likely water). The decision to try alcohols as solvents was based on the fact that they are used to extract fats that consist of long aliphatic chains. These chains are similar to the long aliphatic chains in Adogen. It was found in the literature that hot ethanol and also solutions of 1:2 isopropanol: hexane were used for these extractions.[7]

Table 5 below summarizes the results. The Hansen solubility parameters are included to see if they give an indication of which solvents will be most likely to dissolve the product.

Table 8: Solubility study for Au-MES-Adogen.

		polarity	H.B.	Sol.Para.	Solubility in dried sample	Comments
Au-MES-Adogen		**3.29**	**5.02**	**18.45**		
water		16.00	42.30	47.80	insol	
toluene	bz-CH3	0.74	1.98	18.12	sol	colorless
p-xylene	bz-(CH3)2	0.91	1.83	17.87	sol	turned pink o/n, sm. amt. ppt.
methylene chloride	CH2Cl2	7.74	4.12	20.96	v sl sol	colorless susp.
chloroform	CHCl3	3.10	5.70	19.00	sl sol	colorless susp.
carbon tet	CHCl4	0.00	0.60	17.80	sl sol	colorless susp.
hexane	C6H14	0.00	0.00	15.26	insol	
diethyl ether	$(CH3CH2)_2O$	2.93	5.14	15.68	sl sol	colorless susp.
THF	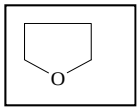	5.69	7.98	19.41	insol	
Acetone	(CH3)C=O(CH3)	10.39	7.04	19.98	sl sol	colorless susp.
Ethyl acetate	CH3(C=O)OC2H5	5.35	7.19	18.13	insol	colorless susp.
NMP	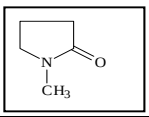	15.60	11.21	23.97	sl sol	turned orange
DMAc	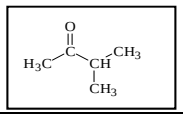	11.47	10.22	22.77	insol	

insol = insoluble, v sl sol = very slightly soluble, sl sol = slightly soluble, sol = soluble

Au-MES-adogen was also tested with alcohols. A 5 ml sample of Au-MES-adogen was dried from toluene, 10 mls of hot ethanol were added to dissolve the dark blue solids, then 20 mls of warm 1:2 isopropanol:hexane were added. A white film formed in a colorless solution. The alcohols were decanted and the white film was dissolved in toluene, although the film was insoluble in water. In time, some blue solids precipitated out. Alcohols appear to react with the excess adogen or perhaps compete with the Au-MES bond (a weak bond). Based on a number of solubility experiments in this study, toluene is by far the best solvent for Au-MES-adogen.

After all the solubility testing and examination of alternate solvents, it was determined that no alternative solvent could, in fact, be used with the same level of NPL compatibility than the toluene, and a new deposition mechanism and/or process needed to be developed. In actuality, much of the deposition development work occurred in parallel with the solubility work, so a successful technique was in fact determined only a short time after it was determined conclusively that only toluene could possibly work.

Several different deposition techniques were tested, each in a lot of 10 or 25 components per technique. These numbers were needed in order to obtain a statistically significant amount of failure or success relative to regular XCOM packaging processes, which have a 50-90% yield range on a lot by lot basis. All technique experimental lots also had control parts in lots of 5 or 10 along with each deposition, build, and test. All in all, about 500 parts were consumed in this work over about a year of time, which is about double the parts and time originally expected. Deposition processes were varied, and devices tested at the die level initially to determine viability. Once viable options were determined, die testing was no longer performed, and parts were assembled blind. Differences were then ascertained based on repeatability and lifetime.

SEM microscopy was used to verify the presence of nanoparticles and estimate removal rate during post-processing. An example contact surface is shown below, with nanoparticles in the 15-50 nm size range. These particles are in the same size range as those seen in the most recent nanoparticle lot fabricated at UDRI, and they are dispersed in a much improved fashion over the clumping of preliminary methods. There are far more particles seen on the lower electrode than on the top electrode, which suggests a different surface state of the two materials. The top electrode may have a metallic difference due to a previously existing adhesion layer that should have been removed as part of the release process. Note that gravity should have no measurable difference at these scales, so any difference between top and bottom electrodes should be entirely attributed to surface states, surface tension, and the toluene and AK-225 drying processes.

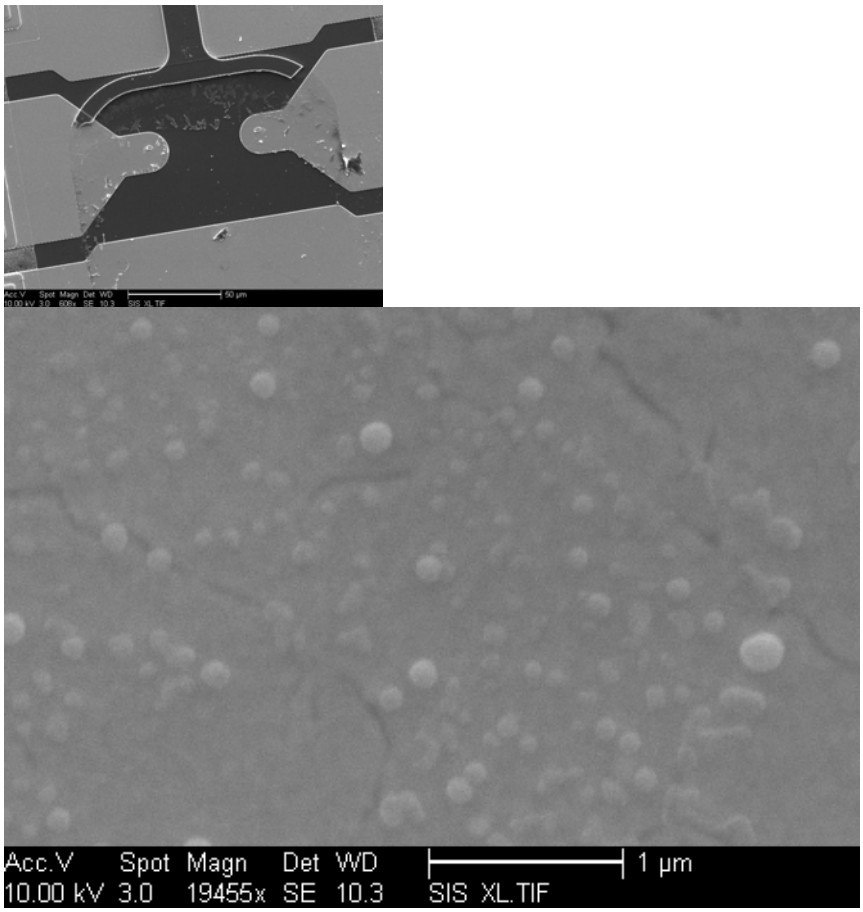

Figure 17: Die region and nanoparticles evident on lower contact electrode.

An early test was to dip the NPL solvent and follow with a soak in AK225. The objective is to see whether the nanoparticles are removed from the surface by AK225. This is of interest because the team determined almost immediately that the solid bridging problem was mitigated with an additional dip in AK225.

After varying dip time and concentration, removal techniques, drying method and time, and AK225 rinsing processes within a reasonable engineering window, a final deposition process was developed in preparation for considerable lifetime and repeatability testing. During the AK225 rinse step, it is estimated (from SEM) that between 75 and 90% of the nanoparticles are removed from the die surface, but that sufficient coverage remains to provide relay electrical performance benefit. The final process is as follows:

1. Retrieve stripped, cleaned, and rinsed known good die from stores (after step 3 of the cleaning process shown on p. 11).
2. Prepare Beaker 1 with 7-10 mm of NPL solution, concentration with OD = 0.29 (the middle concentration of the three samples prepared according to p. 25).
3. Prepare Beaker 2 with 7-10 mm of AK-225, full concentration
4. Manually set all die into Beaker 1 on the lower surface, face up.

5. Let soak for 4-5 min. and remove at a 30-45° angle, setting on beta-wipe. The angle of removal means a low volume of solution will remain on the top surface of the die, and the beta-wipe absorbs a volume of solution from the sides and bottom of each die.
6. Let rest for 3-5 min. to partially dry, then manually set all die into Beaker 2 as before.
7. Let soak for 4-5 min. then remove at a 30-45° angle as before, setting on beta-wipe.
8. Let rest for 3-5 min. to dry, then manually set into chip tray for assembly. The parts may now be stored for up to 24 hours before sealing (possibly longer, unknown).

4.2.2. Task 2, Subtask B – Test Hybrid Packaged Relays

The first part of testing was to develop a baseline suite of data for the exact test conditions examined by this work. A sample test of ten components (20 switching devices) was run to characterize repeatability. The test was performed with 1 mA AC current at a switching speed of 2 Hz (slower rate testing is more accurate for simulating operating conditions) on an HP4338 resistance meter. This test is considered equivalent to low power warm-switching conditions for testing RF components, and is an industry standard test.

One part (with the purple erratic and high resistance contact) is noted as failing this test, and was sent to F/A. This is typical to find components that have some contamination present, and is a normal part of screening and baseline relay performance testing. The remaining components pass, with resistance initially at a moderate level but dropping and settling quickly in the 1.0-2.5 Ohm range. A second part, containing the red device, is considered marginal, but still operates within specification and passes. This test and these results are typical for the XCOM RF MEMS relay product, with an average of 70% of all packaged devices passing this test.

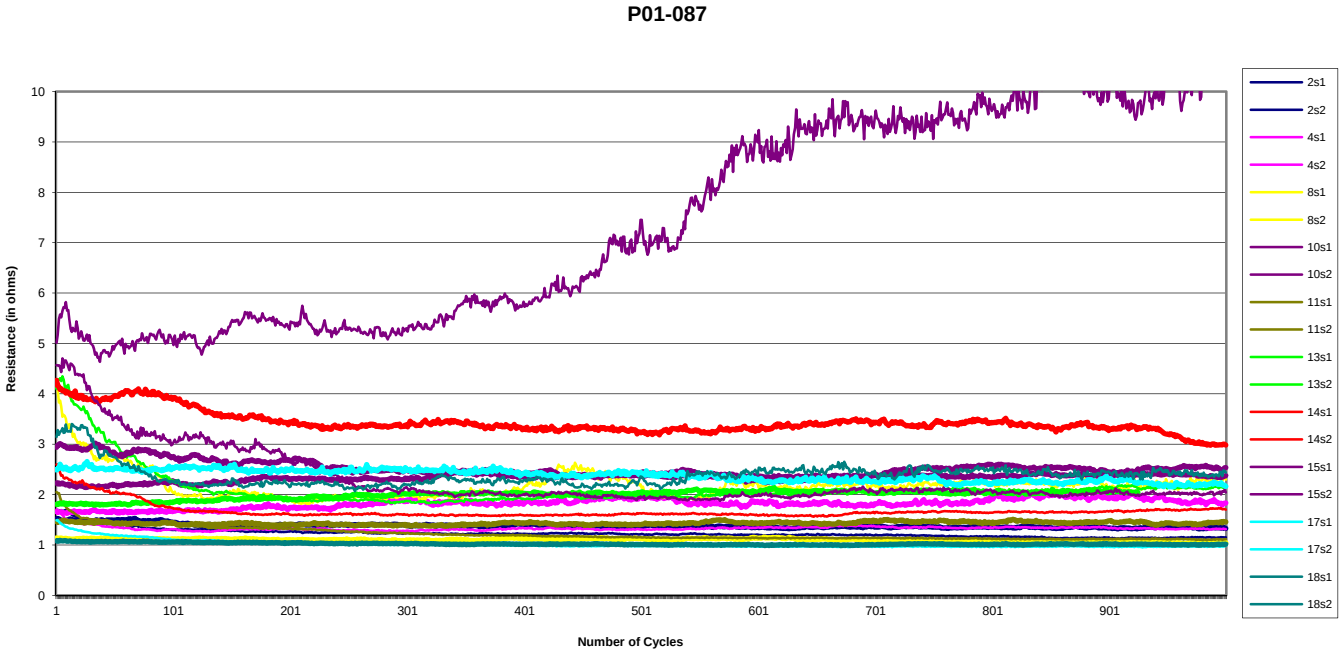

Figure 18: Baseline AC contact repeatability test for RF MEMS relays.

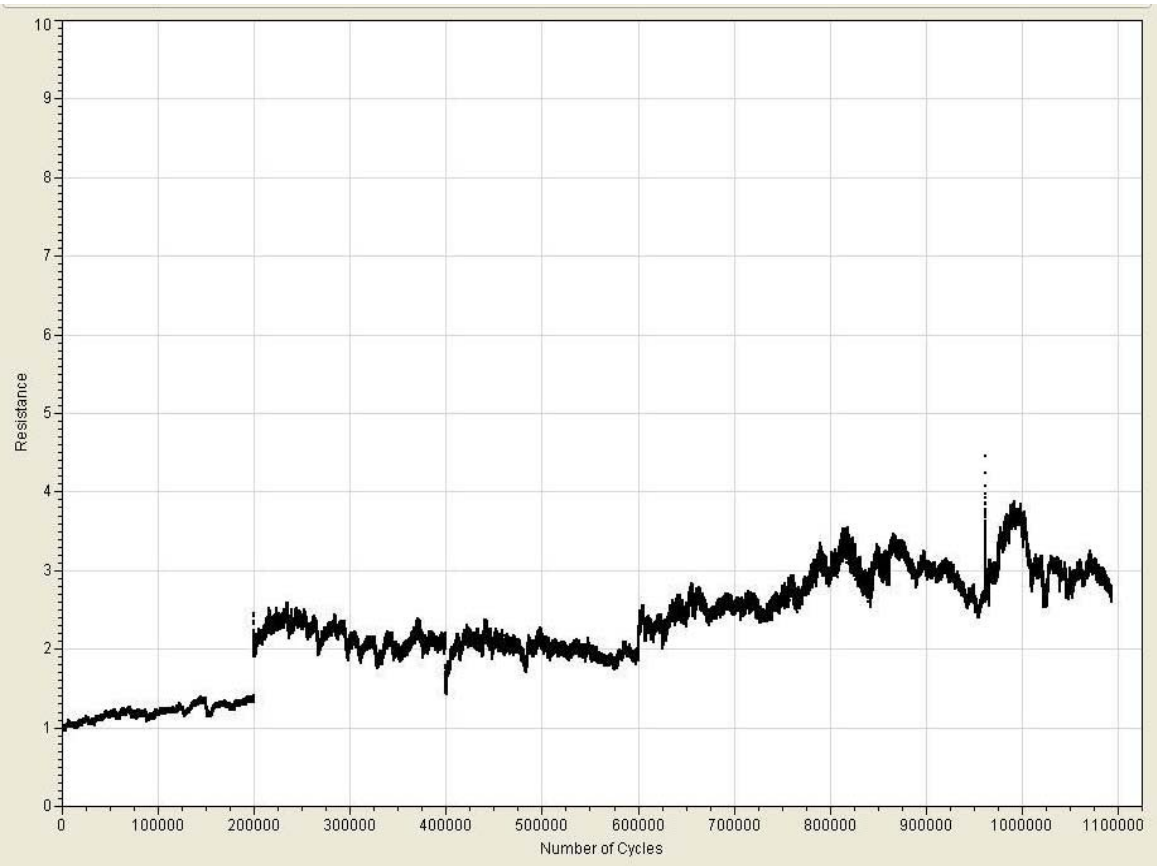

Figure 19: AC contact repeatability for modified RF MEMS relays.

The AC test data suggests that the NPL increases the effective contact resistance under conditions of ultra-low load. This is reasonable to expect, as the contact points are much smaller, although with higher localized pressure. What is interesting in the modified relays is that the contact resistance hits specific plateaus of performance, which evolve over time and use. This suggests multiple nanoparticles are responsible for signal load conduction at any one time, and that the number and pressure on specific nanoparticles can change throughout operation (likely due to the engineered microfrit of the contacts).

The evolution of this low-load condition will need to feed into future models of NPL contact resistance, as these specific test conditions may be dominated by mechanical, rather than electrical or thermal, phenomena. Note that the AC testing does qualify as a "warm-switched" test condition, as the low compliance voltage of 20 uV is on at all times, although it is far too low to cause micro-arcing. It may be large enough to cause liquid bridge formation, or to provide sufficient energy to ablate a nanoparticle, however, and this may be the cause of the evolution of the nanoparticle contacts. If ablation is occuring, however, it is clear from the evolution of the resistance that it is not occuring with every contact make-break operation, or else the plateaus of contact resistance would be unlikely to occur.

The first set of Weibull plots presented is for high-power RF cold-switched lifetime. The parts were switching 2W CW 50-Ohm RF signals at 1 kHz, with both on and off state tested. The data was collected over 12 months of testing, and provides the converged Weibull plots below using Median Rank Regression (MRR) based on the small sample size. The baseline relays showed a characteristic life (officially η, the 63.2% rating on the 50% confidence line) of about 84 million cycles. The NPL-enhanced relays showed lifetime of 135 million cycles, almost double!

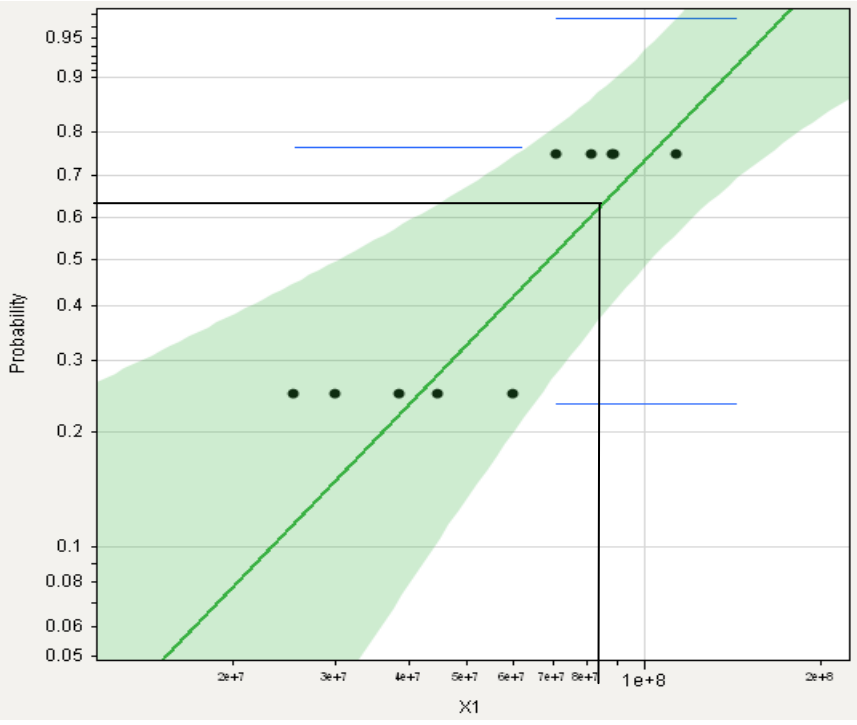

Figure 20: 2W RF cold-switched lifetime Weibull plot for baseline RF MEMS relays.

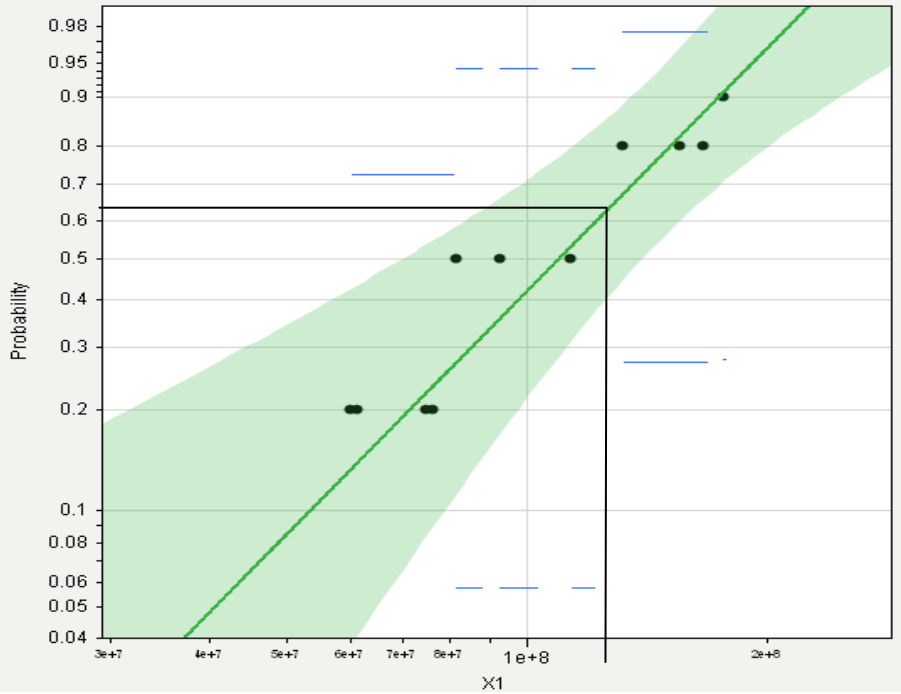

Figure 21: 2W RF cold-switched lifetime Weibull plot for NPL-enhanced RF MEMS relays.

Next is an unconverged Weibull plot for low-power RF cold-switched lifetime. The parts were switching 5 mW CW 50-Ohm RF signals at 1 kHz, with both on and off state tested. The baseline relays showed a lifetime of many hundreds of millions of cycles, without convergence. A single NPL-enhanced relay was tested to 1B cycles and no further testing was performed due to testing time. These values were sufficient to determine there is no likely lifetime problem.

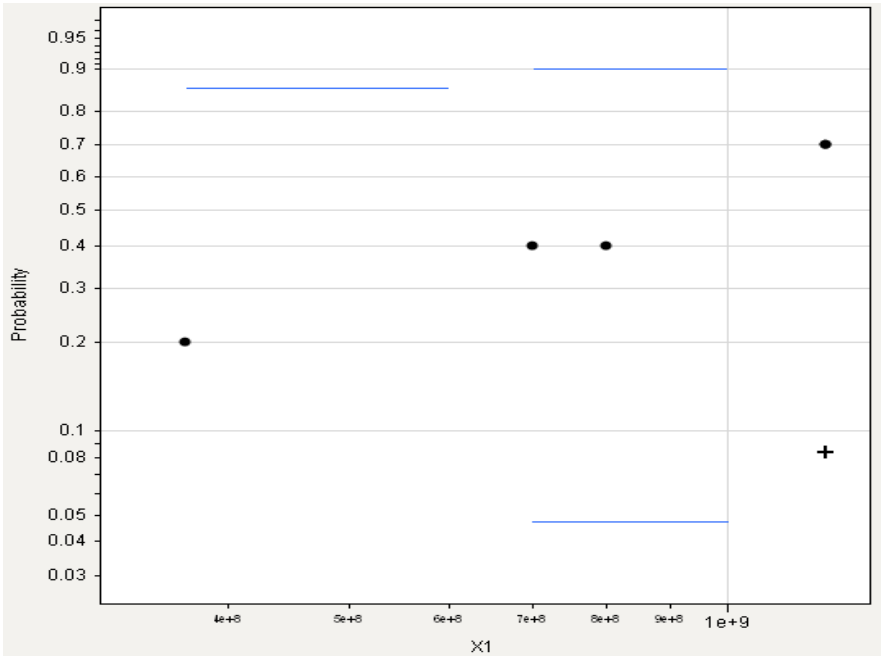

Figure 22: 5 mW RF cold-switched lifetime Weibull plot for baseline RF MEMS relays.

The third set of Weibull plots is for high-power RF hot-switched lifetime. The parts switched 2W CW 50-Ohm RF signals at 100 Hz, with both on and off state tested. The baseline relays showed a lifetime of about 51,000 cycles. The NPL-enhanced relays showed a significant 205,000 cycle lifetime, about a 5x improvement! This condition saw the greatest lifetime improvement, which is in accordance with the theory of liquid bridge collapse damage at the contacts and how the NPL is supposed to mitigate ablative contact material displacement.

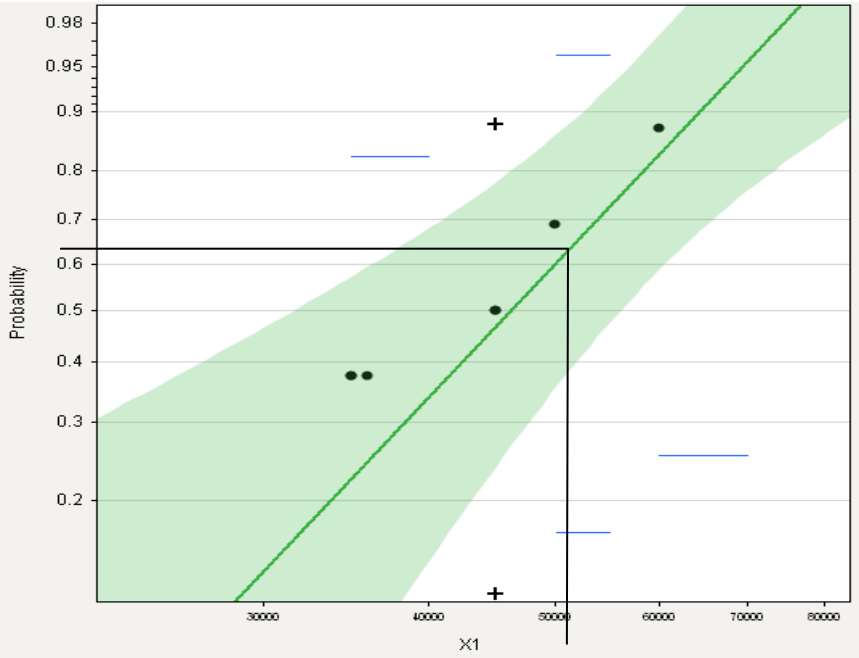

Figure 23: 2W RF hot-switched lifetime Weibull plot for baseline RF MEMS relays.

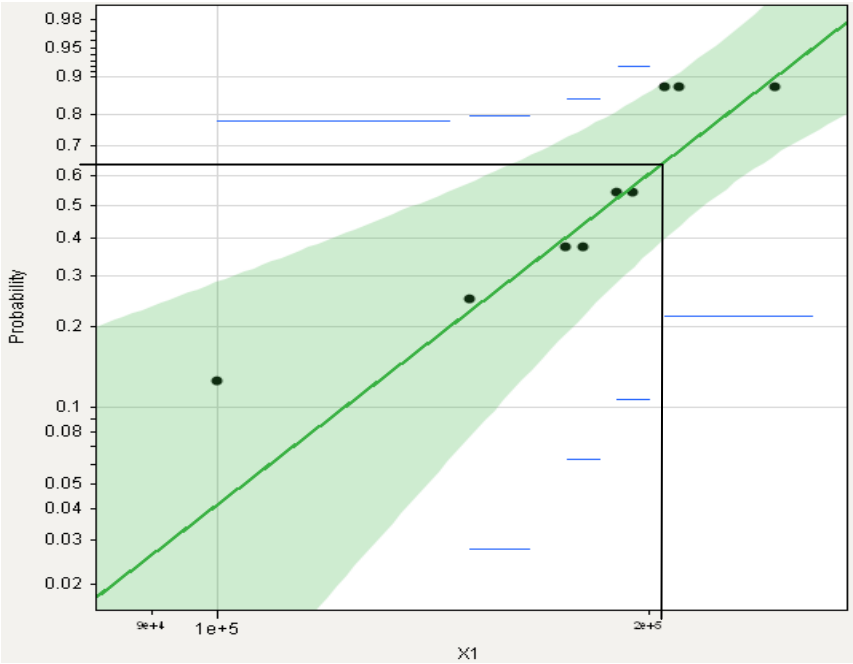

Figure 24: 2W RF hot-switched lifetime Weibull plot for NPL-enhanced RF MEMS relays.

The fourth set of Weibull plots presented is for low-power RF hot-switched lifetime. The parts were switching 5 mW CW 50-Ohm RF signals at 100 Hz, with both on and off state tested. The baseline relays showed a lifetime rating of about 420,000 cycles. The NPL-enhanced relays showed a significantly improved 700,000 cycle lifetime, about a 2x improvement.

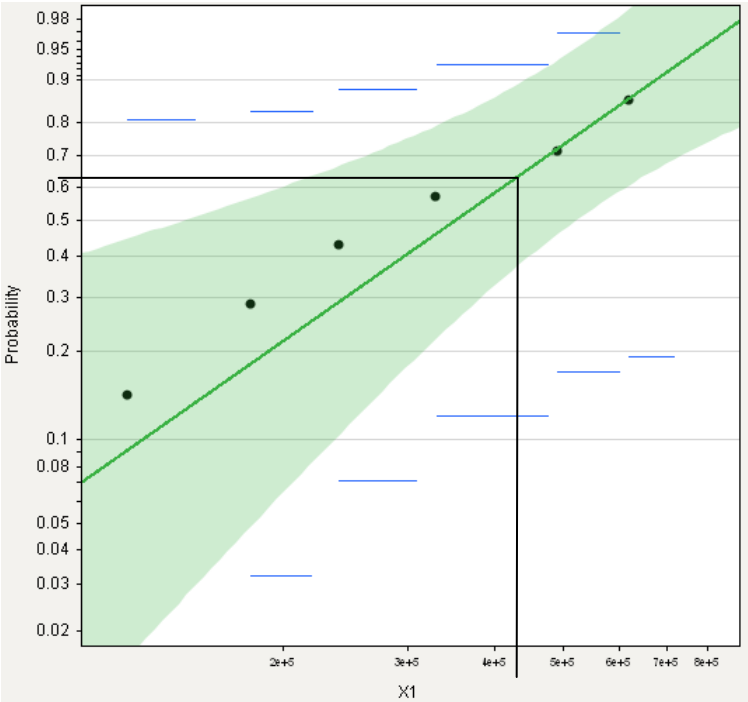

Figure 25: 5 mW RF hot-switched lifetime Weibull plot for baseline RF MEMS relays.

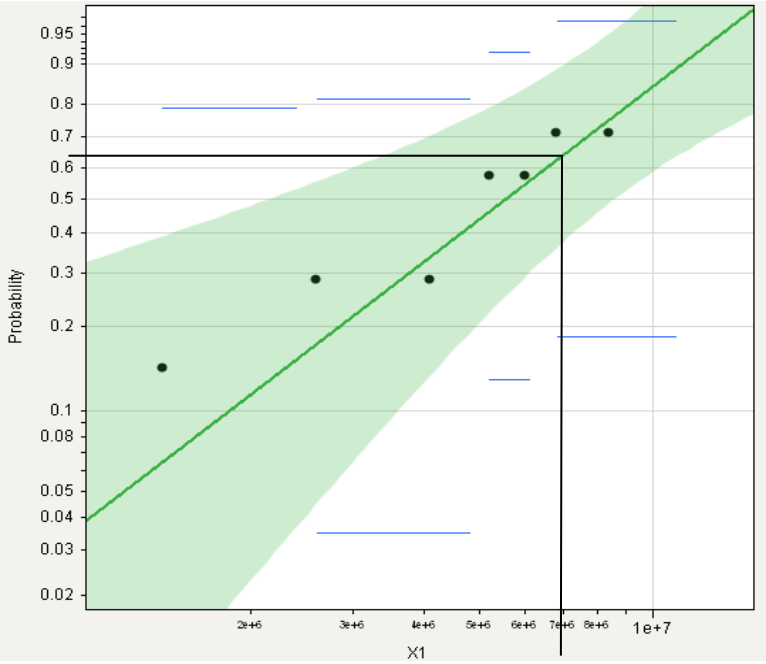

Figure 26: 5 mW RF hot-switched lifetime Weibull plot for NPL-enhanced RF MEMS relays.

The Weibull plots provide a great deal of analysis with respect to the lifetime of the parts, and what that expected lifetime range and deviation is likely to be. As more data is collected, the confidence level in the plot improves and the results become more accurate. In general, about 6 data points were required to converge each plot, providing sufficiently high confidence levels. Future work in longer lifetime enhancements should strongly consider parallel component testing, in order to turn a year or more of required data collection into a few months, and enabling 10-20 data points per condition. It is surmised that variations in NPL deposition (and potentially toluene-enhanced contamination) on a part by part basis may have contributed to the spread of component performance wider than that experienced by the baseline components.

The table below summarizes the characteristic lifetimes for the different conditions as compared to the initial baseline expectations and goals at the start of the program. What is seen is that the baseline expectations are within the range of actual data, which should not be surprising given that early DC testing generally correlates well to RF power handling results in cold-switched conditions. The baseline RF hot switch performance is slightly better than predicted.

Table 9: Summary of lifetime test data for NPL and control parts vs. initial goals

Specification	Conditions	Est. Baseline	**Baseline**	NPL Goal	**NPL**	Units
Cold Switched	at 40 dBm, 50 Ohm	10^4 to 10^6	-	10^8		cycles
	at 33 dBm, 50 Ohm	10^7 to 10^8	**8.4x10^7**	~4x10^8	**1.35x10^8**	cycles
	at 30 dBm, 50 Ohm	10^8 to 10^9	-	10^9		cycles
	at 7 dBm, 50 Ohm	10^8 to 10^9	**~7x10^8**	~1x10^9	**~1x10^9**	cycles
Warm Switched	at 20 dBm, 50 Ohm	10^3 to 10^4	-	10^6		cycles
	at 10 dBm, 50 Ohm	10^4 to 10^5	-	10^7		cycles
	at 7 dBm, 50 Ohm	10^4 to 10^5	**4.2x10^5**	~1x10^7	**7x10^5**	cycles
	at 0 dBm, 50 Ohm	10^5 to 10^6	-	10^8		cycles
Hot Switched	at 40 dBm, 50 Ohm	0	-	10^2		cycles
	at 33 dBm, 50 Ohm	10^2 to 10^4	**5x10^4**	~1x10^5	**2x10^5**	cycles

The most important data in the table is the lifetime improvement seen in the NPL-coated parts. In the cold-switched case, the lifetime approximately doubles, which is a critical asset for present commercial customers in the automated test equipment and industrial switching space. The previous lifetime of 84 million cycles for high-power switching is now 135 million, which results in significant cost savings for test equipment manufacturers running long-life relay boards (100 million is considered a critical lifetime plateau). This is a commercial boon, and will result in XCOM licensing the Air Force NPL technology for use in the commercial sector.

The improvements are even greater in the hot-switched cases, with sufficient data taken to prove the increase is real with high confidence. The lifetimes increase by a factor of two times at the low power condition, and five times in the high power condition. This is a major improvement, although it is less than the 10-100x seen in the laboratory testing performed at UDRI.

4.2.3. Task 2, Subtask C – NPL Deposition for Wafer-Scale Packaged Relays

In this Subtask, NPL candidates were to be applied in a deposition process compatible with IMT's release and cleaning process as part of the Xipe-Totec wafer-scale packaging used for XCOM and Harris tuning and filter circuits. This Subtask began prior to the availability of NPL material due to supplier timing and was completed at the same time as Subtask 2A, which ensured compatibility with the final manufacturing steps in the Xipe-Totec process.

After significant process development that occurred during the first year of the program, the first wafer scale packaged components were fabricated through to the point of completing all intended elements. Sample microphotographs are shown below, with contamination evident and requiring analysis. Electrical testing showed that no devices were functional.

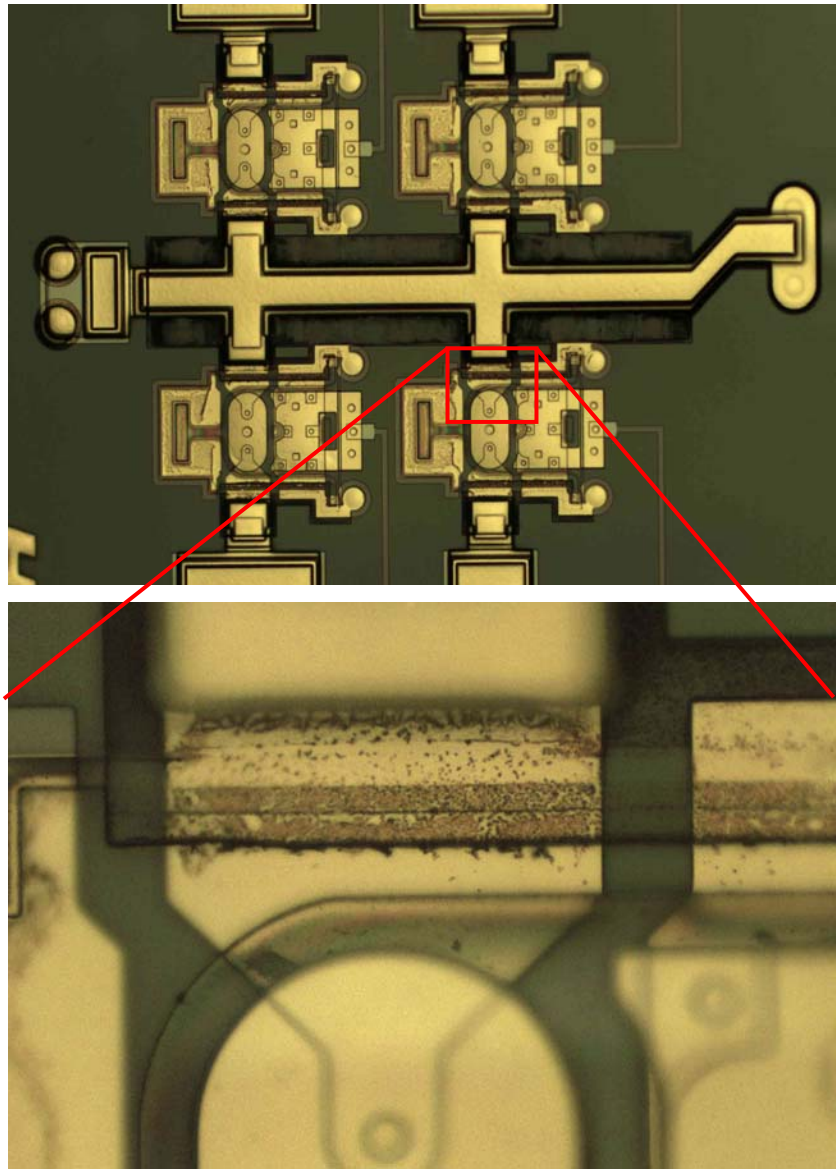

Figure 27: Wafer-scale packaged RF MEMS tuning circuits showing contamination.

An incompatibility between the thick plating layer (and initial plating seed layer) and underlying oxide and gold layers was examined by SEM. The overlapping of the two oxide delineation steps resulted in trapped plating seed along sidewalls. The trapped material interacted with later wet chemistries to form a polymer-metal stringer that shorted most metal surfaces together, and added to organic contamination due to etchant traps. The entire wafer was then subjected to 1.5 min ion milling, with half subjected to 6+ min at 45° angle. Correlating SEM with optical microscopy shows that stringers and contamination regions are both readily visible, and that ion milling was unable to remove the material.

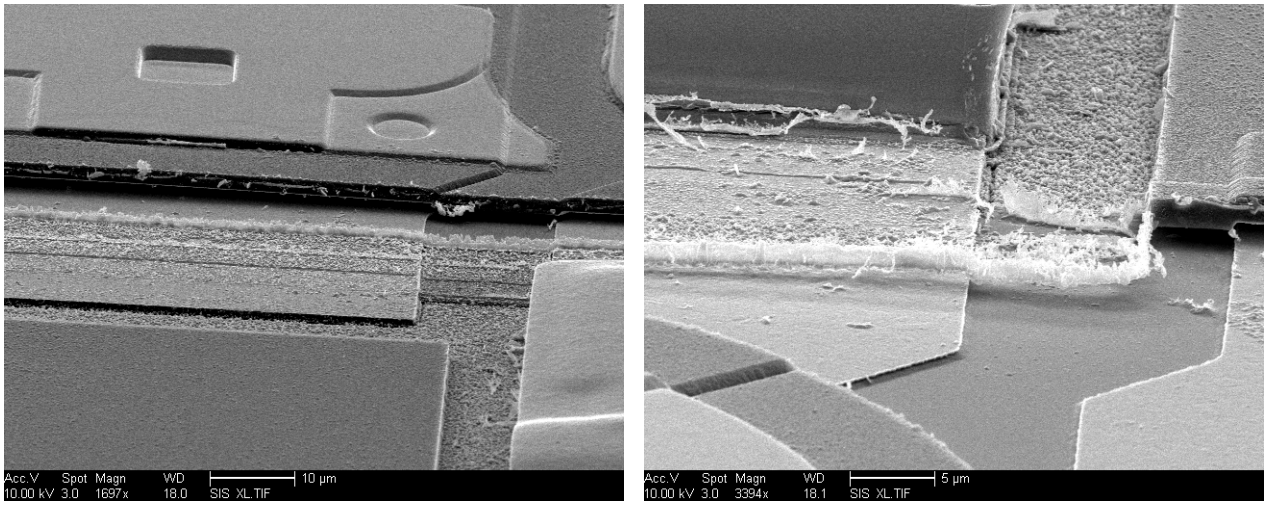

Figure 28: Die with 1.5 minutes of ion milling; stringers still remain, and adding surface damage.

Two samples were IEDX examined to examine the materials present in the stringers. One sample was coated with thin iridium to eliminate charging effects for SEM work, and the other was tested without iridium to eliminate potential peak interactions. What is determined is that the stringers contain primarily carbon, oxygen, gold, and silicon, which is consistent with the plating base and polymer recombination from wet processing.

Table 10: IEDX Results for wafer-scale process incompatibility.

Spectrum processing : No peaks omitted
Processing option : All elements analyzed (Normalized)
Number of iterations = 4
C CaCO3 1-Jun-1999 12:00 AM
O SiO2 1-Jun-1999 12:00 AM
Si SiO2 1-Jun-1999 12:00 AM
Ir Not defined 1-Jun-1999 12:00 AM
Au Au 1-Jun-1999 12:00 AM

Element	App Conc.	Intensity Corrn.	Weight%	Weight% Sigma	Atomic%
C K	2.47	0.4544	6.16	1.15	32.54
O K	3.77	0.6031	7.09	0.83	28.14
Si K	5.83	1.1373	5.82	0.25	13.16
Ir M	8.34	0.8933	10.60	1.12	3.50
Au M	50.98	0.8231	70.32	1.45	22.66
Totals			100.00		

The contamination was determined to contain a variety of organic and metallic materials that would not enable the type of final sealed cleanliness required for proper operation and repeatability at high power levels, so a significant process change was required to eliminate the problem. The thick plated layer was replaced with a lift-off 2 um gold layer, which increased overall resistance, but eliminated the risk of plating process contamination. This enables the use of high-Q passive capacitors, but eliminates the ability to fabricate high-Q passive inductors of significant size. This means integrated filter banks would be compromised, but amplifier tuning circuits could still have full capabilities.

By the end of the program, the wafer-scale packaging run was able to complete two device wafers to the point of release. Both of these final wafers suffered delamination of high-voltage electrode films under the stress of electrostatic actuation. It is postulated that either the release was over-etched, or that the electrode films were deposited without any adhesion metal due to foundry error. At that point, cost and time over-runs forced an end to the project. It can be revisited at any time, but only for a major program and customer requiring fully integrated filter and tuning circuitry with the lowest possible loss. In the meantime, alternative wafer-scale packaging techniques are already underway with a much lower-cost provider, and those will be used to continue wafer-level NPL deposition work.

Despite the process difficulties with the top two layers in the integrated wafer-scale packaging process, the NPL deposition technique was designed based on the hybrid deposition technique. Process glassware and fixturing was identified at IMT, and a process control document prepared. The process was run at XCOM first on test wafers without microstructures using equivalent fixturing and toluene without NPL present. Deposition appeared to be equivalent without pooling, although the process was never tested on a full device wafer

1. Complete release and rinse of device wafer as normal; do not remove from wafer holder
2. Transfer to adjacent development hood and attach wafer holder to NPL dip fixture
3. Start NPL dip fixture. It will automatically dip the wafer at a 15° into the NPL solution
4. The fixture will soak the wafer for 5 min under very slow stir agitation (setting 1.5)
5. The fixture will automatically remove the wafer at a 15° angle and hold for 3 min
6. The fixture will then rotate to a second bath and dip the wafer at 15° into AK225
7. The fixture will soak the wafer for 5 min without agitation.
8. The fixture will automatically remove the wafer and hold for 3 min
9. The fixture will then present the wafer back to the operator for removal and bonding

In the new wafer-scale process, IMT would then tape-mount the wafer in nitrogen and ship to the new wafer-scale package supplier for bonding.

4.2.4. Task 2, Subtask D – Test Wafer-Scale Packaged Relays

This Subtask was to test wafer-scale packaged components in the same manner as the hybrid versions. No wafer-scale packaged components were completed during the period of performance, despite the addition of over $1M in internal R&D funding from both XCOM and Harris. A variety of costly process incompatibilities prevented delivery of completed wafers for dip testing with the developed process.

4.3. Task 3 – Demonstrate Improved Efficiency

The power amplifiers (P/As) in tactical radios can operate as high as 60-70% efficiency, but in reality operate at 20% or worse in the field.[8] Significant power is wasted because the P/A does not adapt to changing operating conditions. As next-generation radios seek to support 4-G, 802.11g, MUOS, WiMAX, MUOS, Soldier Radio, WIN-T, and other waveforms, battery life problems will be exacerbated, increasing cost, size, weight, and power needs.

Early laboratory experiments demonstrated that 50%+ efficiency can be maintained across a wide range of operating conditions if the biasing control and matching circuits adapt and tune. Unfortunately, the tuning quality factor (Q) required is impossible to achieve with semiconductor technologies, so developers are looking to RF MEMS for low-loss tuning and switching. This task was to develop a tunable P/A, enabling optimal efficiency over a wide frequency range.

Due to cost and time over-runs in the first two tasks, this development thrust could not be performed supported by this program. Fortunately, XCOM was able to perform different power amplifier work under a Navy program that is still relevant to the overall product goals of the Air Force. The complementary Navy program is N66001-10-M-1005, which is a Phase I SBIR. One major difference in the Navy program is that the interest was in tuning over changing antenna conditions but with a fixed waveform and frequency band (280-320 MHz MUOS satellite link).

Selected relevant results are presented here, though only about 1/3 of the material presented was supported by internal XCOM R&D funds and could be considered a direct cash investment towards this program. The remaining 2/3 are the results of the Navy program.

4.3.1. Task 3, Subtask A – Design Tuning Circuit

The matching circuits must provide instantaneous full bandwidth with varying desired output power and operating conditions (environmental and RF). Efficiency is valued over cost and complexity, but compact size (weight, cost) is a real engineering limitation due to the desired speed of product development and testing. General specifications are as follows:

- DC-RF Efficiency: 50% or better throughout the majority of operational states
- Input Impedance: 50Ω (likely fixed)
- Output Impedance: 50Ω (modifiable between 25 and 150Ω to accommodate hand or body proximity, horizontal position, antenna damage, use inside vehicle, etc.)
- Power Output: 8 watts (39 dBm) with 1 dB compression (negligible distortion)
- Frequency: 280 MHz to 320 MHz (300-320 most critical initial band)
- Accommodate legacy notched WCDMA signals (low bleed/fill)
- Initial size “soft goal” is 1.5 in^2 (without control electronics or optimization)

An integrated wafer-scale packaged tuning circuit was designed to fit within a ladder impedance matching architecture. Metal-Insulator-Metal (MIM) capacitors with silicon nitride as the dielectric film is selected due to ease of interconnect and thin-film compatibility. The integrated device has switched capacitors, with two designs created. The first design is a single tuner chip with three bits of capacitance selection. The second design is a dual tuner chip with two capacitors each with two bits selectable, as seen in the mask layout below.

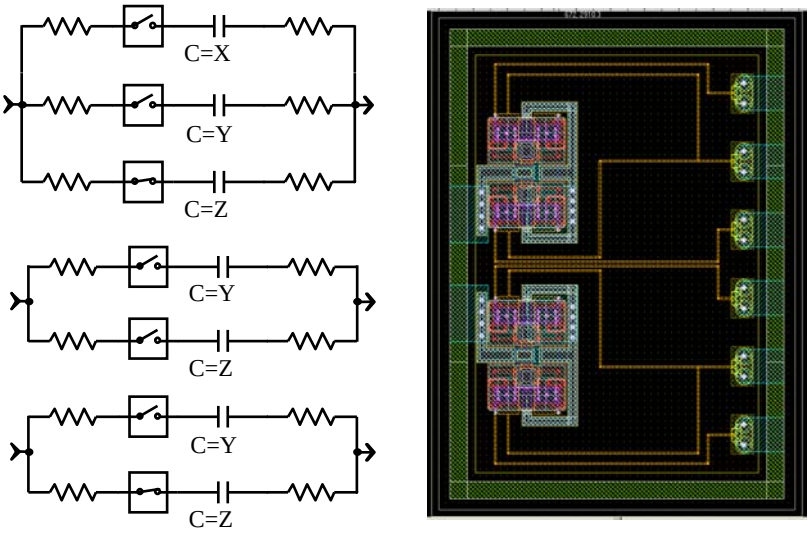

Figure 29: Circuit diagram for 3-bit and dual 2-bit tuners, and wafer-scale layout for dual 2-bit tuner.

The designs for the integrated tuners were selected for ladder tuning networks requiring lower capacitance values but with a high sensitivity to inductor variance. The values required are low, only requiring single digit pF tuning in order to have large swings in impedance matching. The 3-bit tuner is designed with X = 0.5 pF, Y = 1 pF, Z = 2 pF. The 2-bit tuner is designed with each having Y=1 pF and Z = 2 pF, and a fixed 1 pF capacitor shunting in parallel.

The hybrid circuit was designed for much larger capacitance values that could be modified on the fly during the testing stages. The simplest circuit designed early in the Phase I effort would use the standard XCOM component as a switch for a pair of chip capacitors to ground. The higher ESR of the part (1 Ohm) was somewhat mitigated by the lower ESR (0.1 Ohm) of the high-quality chip capacitors available from Passive Plus, Murata, and other vendors.

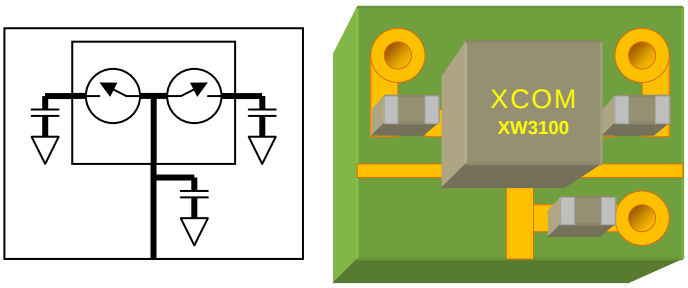

Figure 30: Architecture for remaining hybrid tuning circuit design

The initial design phase suggested that values in the 2-100 pF range covered a variety of P/A architectures and designs. Typical tuning was performed by manual tunable capacitors in the 2-37 pF range atop other fixed capacitors. After examining different designs and analyzing the manufacturer's data for different chip capacitor vendors, the following chip capacitors appear to best suit our needs for this specific tuning circuit design.

Passive Plus (www.passiveplus.com)
High-Q/Low ESR 0805 250V line
Values 0.7, 1.3, 2.4, 4.3, 9.1, 18, 39, and 62 pF

Emboldened by early success, the complexity of the tuning circuit model was then increased, and the transmission line design was revised into discrete lumped elements with separate tunable and fixed capacitor elements. Resistance was added to account for MEMS hybrid tuning elements, assuming 1 Ohm per switching point as shown below.

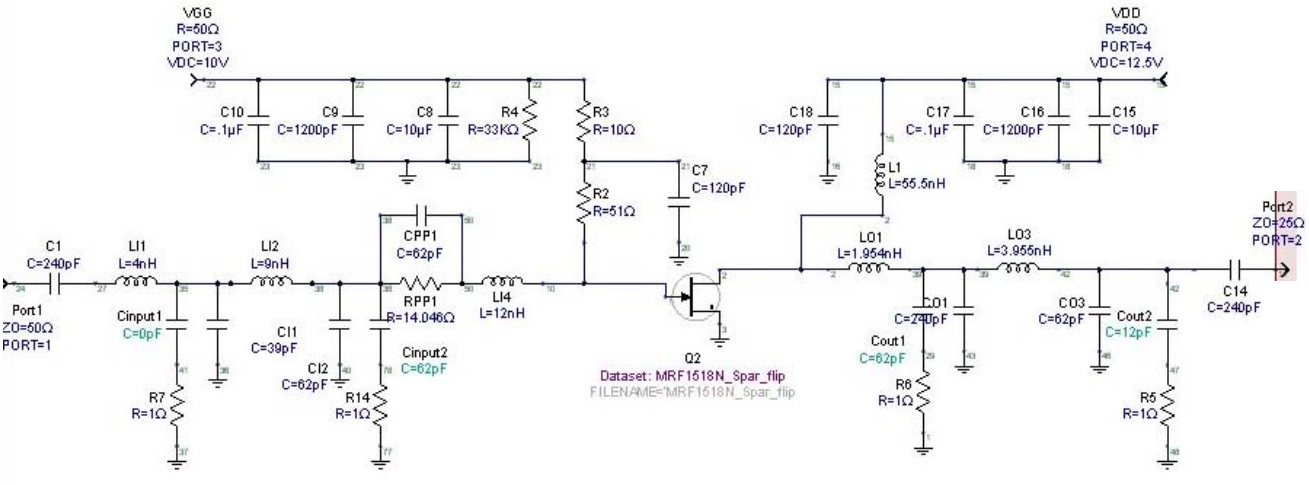

Figure 31: Revised model with greater detail on tuning circuit.

The model below shows P/A output gain at high power when the output is varied to 25 and 150 Ohms. The original 65% PAE drops to 55/43% at 25/150 Ohms output. The second model shows that switching in a single large value 62 pF capacitor at one tuning point recovers the 25 Ohm case well, with an equivalent overall power envelope in-band. Such a value would be difficult with many technologies, but the hybrid tuner can accomplish this easily and compactly. It was also demonstrated that a 34 pF capacitor switched in at the same tuning point recovers the 37 Ohm case, proving that detuning and tune recovery operates in a somewhat linear fashion.

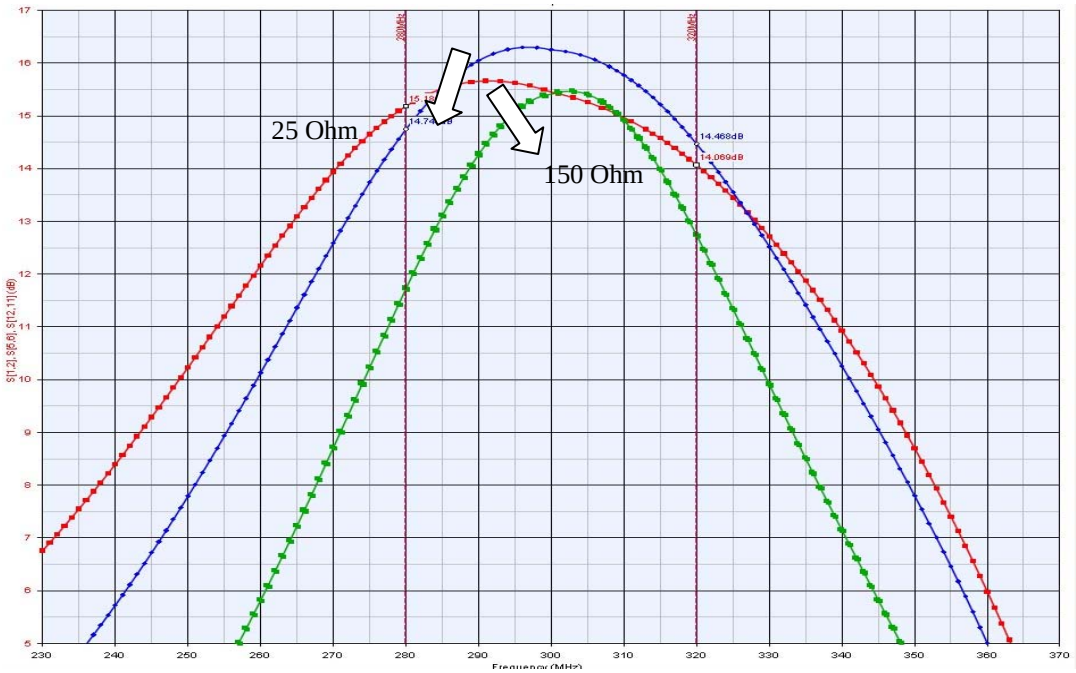

Figure 32: Amplifier de-tuning due to impedance mismatch with antenna.

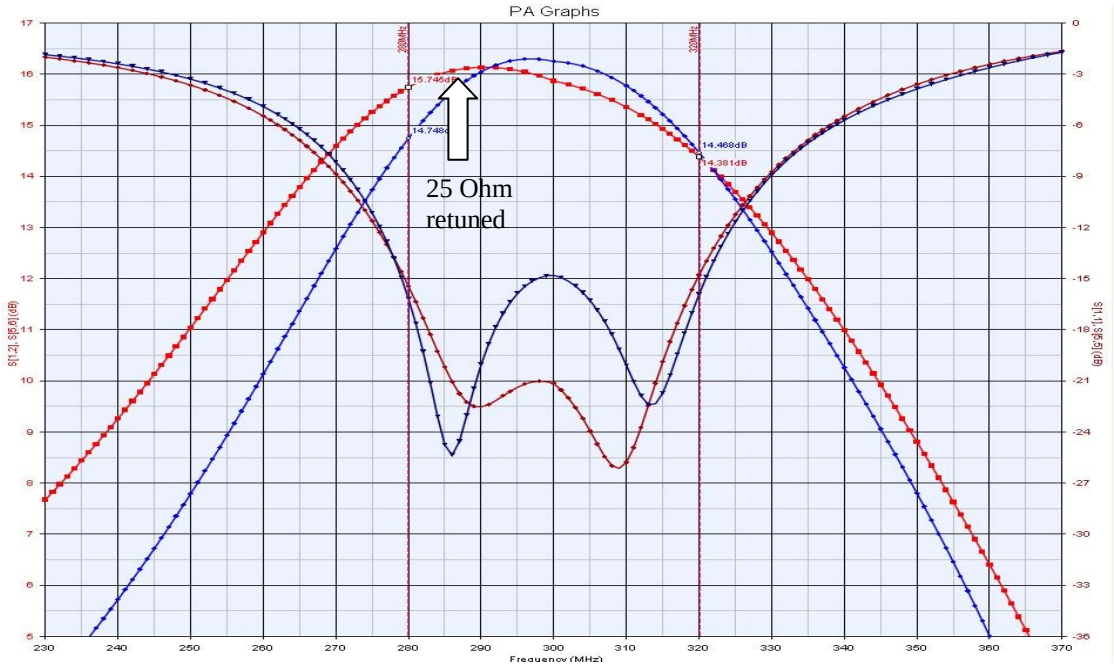

Figure 33: P/A model showing de-tuning drop and RF MEMS tune recovery for 25 Ohms.

The 150 Ohm case was harder to tune using only switched capacitors in the tuning circuits. The bandwidth narrowed, resulting in only 57% final PAE, although it could be centered anywhere in band. The addition of a 1.5 nH chip inductor would broaden the peak, but add loss (0.3 dB) and potential signal leakage/contamination. The design assumed capacitor ESR of 1 Ohm, achieving 60%+ PAE. If tuners are 3 Ohms ESR, then P/A gain drops by 1 dB, causing 60% PAE to drop to 48%, which validates the weakness of semiconductor tuning in the literature. Overall, this first design proved the models are reasonable, the tuning concept is viable, larger capacitance is attractive, and ESR is critical.

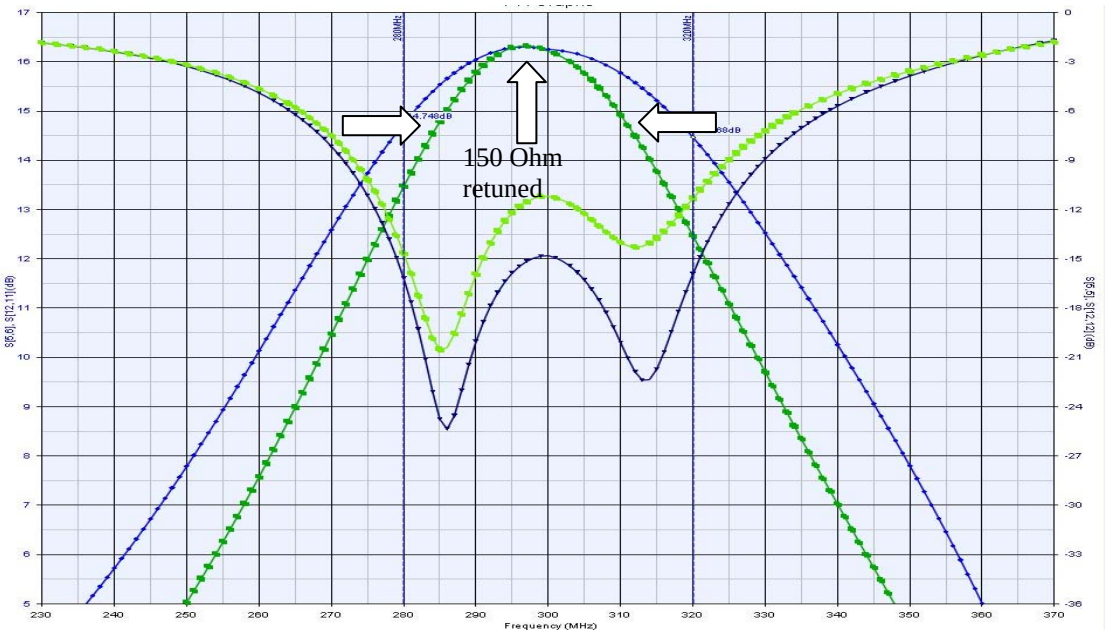

Figure 34: P/A model showing de-tuning drop and RF MEMS tune recovery for 150 Ohms.

4.3.2. Task 3, Subtask B – Assemble Amplifier Circuit

In this subtask, the full P/A is fabricated, assembled, and tested. This task moves into higher power testing, where the characteristics of the transistor change and must be adapted for in order to maintain efficiency. A redesign improved the resonance modeling from data collected during the middle of the Navy program, and recommended subtle via placement improvements and fixed capacitor value adjustments. It should be noted that gain values were not as high as modeled in initial tests, so design improvements continued through the end of both programs for better matching, heat sinking, and biasing conditions to optimize higher power testing.

The Navy final review emphasized power testing concerns, as well as additional reliability tests to be considered for any future work. The primary goal by the end of the Optional effort was to be a second closing of the design loop, enhancing the accuracy of all models, and enabling the modeling of alternative biasing to address efficiency for varying output power.

The fifth revision of board artwork in the Navy program was completed, and a low-cost laser-print and transfer rapid-prototyping process was used. This is not the same amplifier as shown in the design work above, but a simplified version with only three matching nodes instead of five. Note the active area of the board is only ~2 in^2 including bias circuitry, even though neither the bias nor matching circuit has been optimized for size. This is about 1/3 the size of present MUOS amplifiers. The combination of transmission lines and lumped elements keep quality factors high but size relatively compact.

The original plan was to use a commercial board supplier to provide higher quality vias and heat sinking, but these advantages were exchanged for speed in support of continuous iteration and adjustment. The “quick and dirty” sub-optimal vias and pads are compensated for in the circuit model, so only heat sink performance is actually sacrificed. After Navy review, the boards were modified and bolted to commercial air-cooled machined aluminum heat sinks to increase power handling. Higher power bench-top test equipment was characterized, with a pre-amplifier to increase input power levels, and then attenuators follow before the network analyzer. The necessary components were characterized and assembled.

It is important to note that this amplifier design is not actively switched with RF MEMS tuning circuits. It is fully fixed in its designs, with the capacitor values replaceable manually through solder/desolder operations. There was insufficient time and funds to add the MEMS to the hardware prototype, so the hardware assembly and test is to assess the P/A itself and its limits.

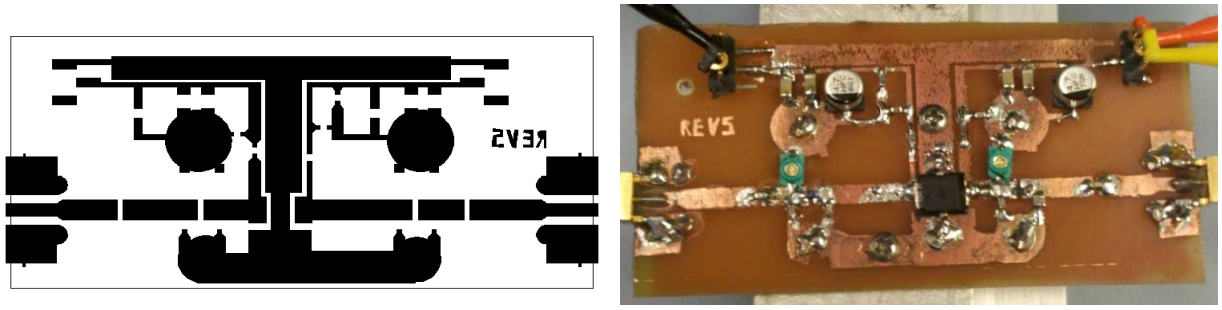

Figure 35: First full P/A artwork and assembled board under test.

4.3.3. Task 3, Subtask C – Test Amplifier Circuit

The P/A was set up on the bench top with the input side having biasing power supplies and a COTS benchtop pre-amplifier, provides up to 1W input. The DUT was on an aluminum fin bar. The output side has a pair of attenuators (~–60 dB at passband) and power meter for accurate gain measurement. Consumed power was directly measured for accurate efficiency calculations.

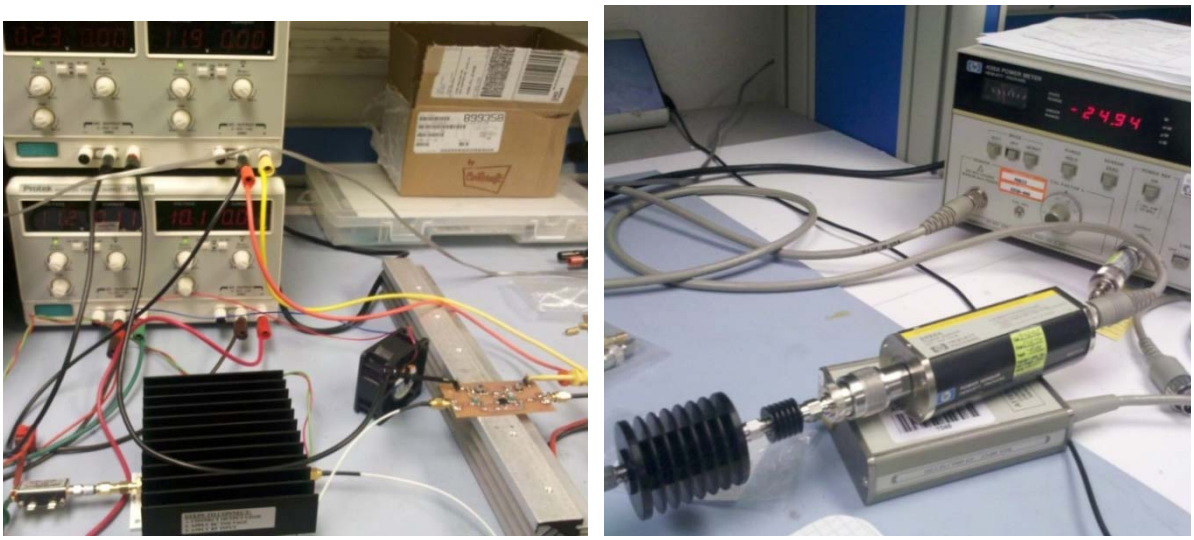

Figure 36: Bench-top high power test set showing input and output chains.

A laser doppler temperature meter was used during power testing. At output of 1 Watt continuous wave, the steady state transistor package top temperature was 31 C (shown right). The source pad ~2 mm away from the transistor was at 36 C, which more accurately reflects the temperature seen inside the component, as this metal trace is sourcing the full current, and is responsible for pulling heat away from the part.

At 6 Watts, the steady state transistor temperature was at 45 C on the package top. The source pad was at 65 C, which is approaching a safe operating limit! Efficiency will already start to decline by the time this temperature is reached.

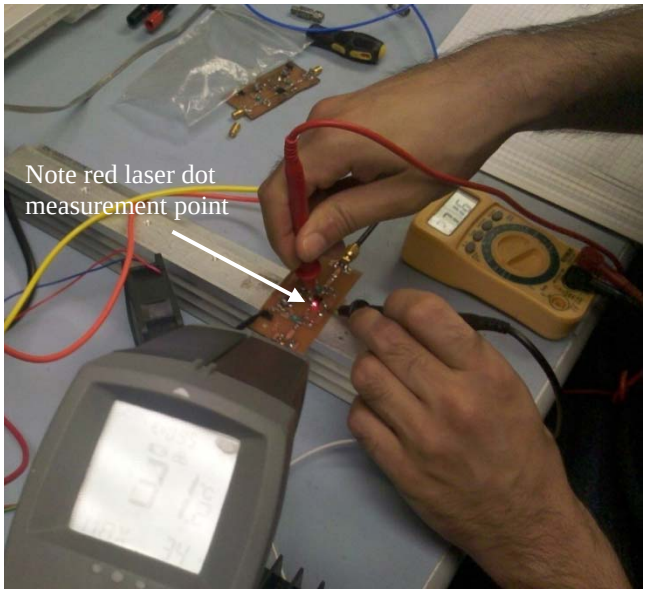

Figure 37: Temperature measurement of P/A under test.

Testing determined a maximum power of 6W, as limited by a 1.5A DC current power supply, and effectively hampered by thermal transport. Contrary to initial concerns, the RF output inductors handled 6W without any temperature rise, so transistor source temperature is the real constraint. Improved vias will definitely improve efficiency & maximum power, as it would keep the temperature down, enabling the full 8-10W out for 1.5A in (as ref designs). The signal path can also be improved with thicker metal for another 0.5-1dB of gain and higher efficiency.

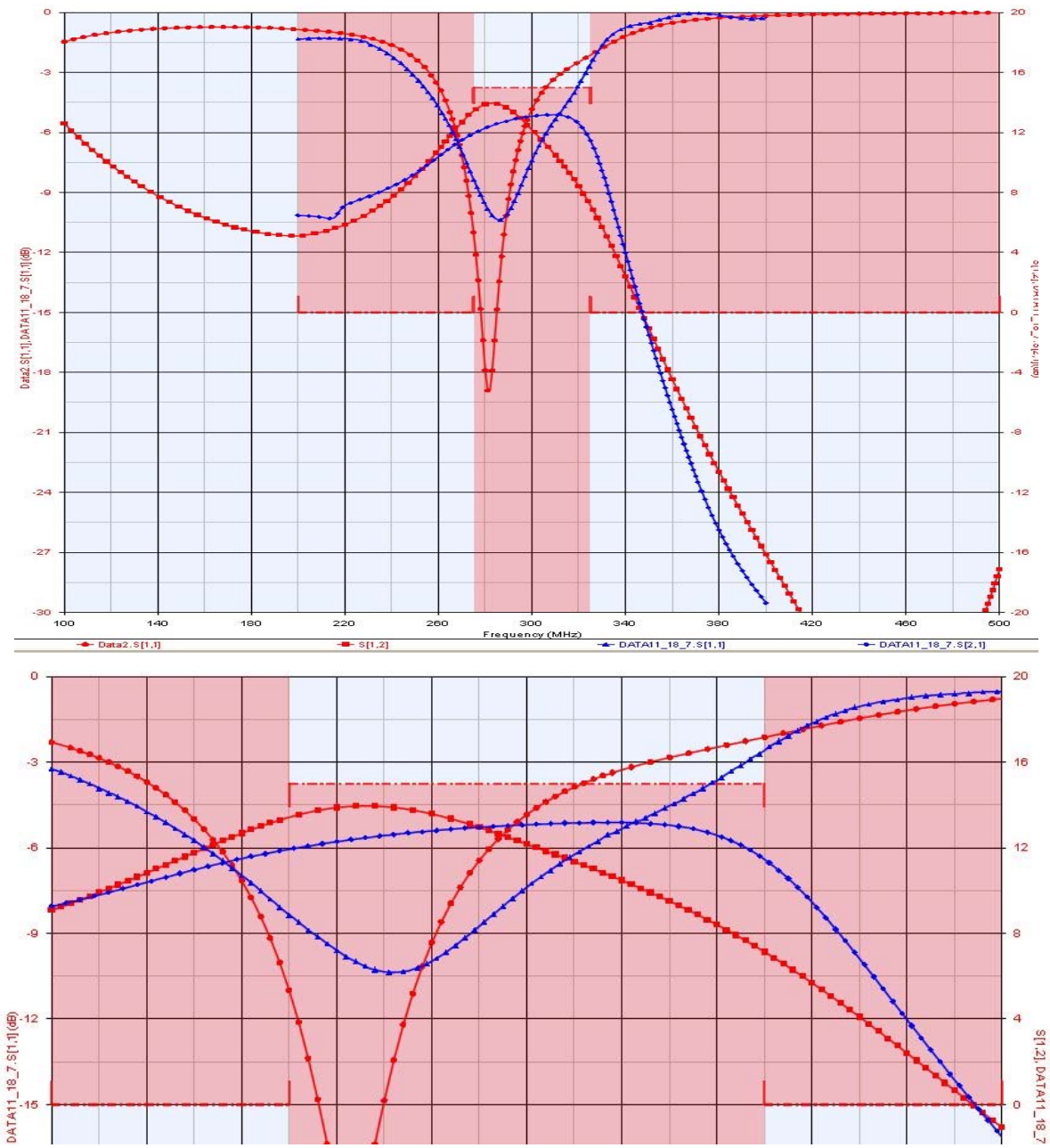

Figure 38: Broad and zoomed views of P/A data (blue) and model (red) small-signal test.

A total gain of 12-13 dB was seen across the full band during the small signal test. The bias and tuning conditions were as follows, with tuning conditions maximized for low output power. This same matching also works moderately well for the mid-range power of 1-2 Watts.

- Vdrain = 12V
- Vgate = 2.4V
- Iq = 180 mA
- TrimIn = 17 pF
- TrimOut = 7 pF

The transistor small-signal characteristic data and S-parameter-based experimental data is accurate for lower power designs, but using these models at high power is not accurate. The

following plot shows data for the small signal test (black curve) along with the mid-power and high-power tests. As the power was increased, the gain dropped as the P/A went out of tune, and the transistor heated up. This proves that a refined experimentally-determined SPICE-based model needs to be used for the next substantive iteration.

The lower two curves (with dot data points) show efficiency as directly measured and including RF input power. The power added efficiency at 6 Watts output was in the 40-55% range, which is not far from the Navy's goal of 50% across all conditions. It is clear that increasing output to 8 Watts while using the same 1.5A source current would enable the target modeled 70%+ PAE. As output power drops to the 1-1.5W range, PAE drops to about 25% as is typical for simple Class B amplifiers (see Fig. 39). This mid-power data is perfectly consistent with expectations, and validates our assertion that the small signal design process works well for low-mid powers, but breaks down at higher powers (and with non-linear temperature effects).

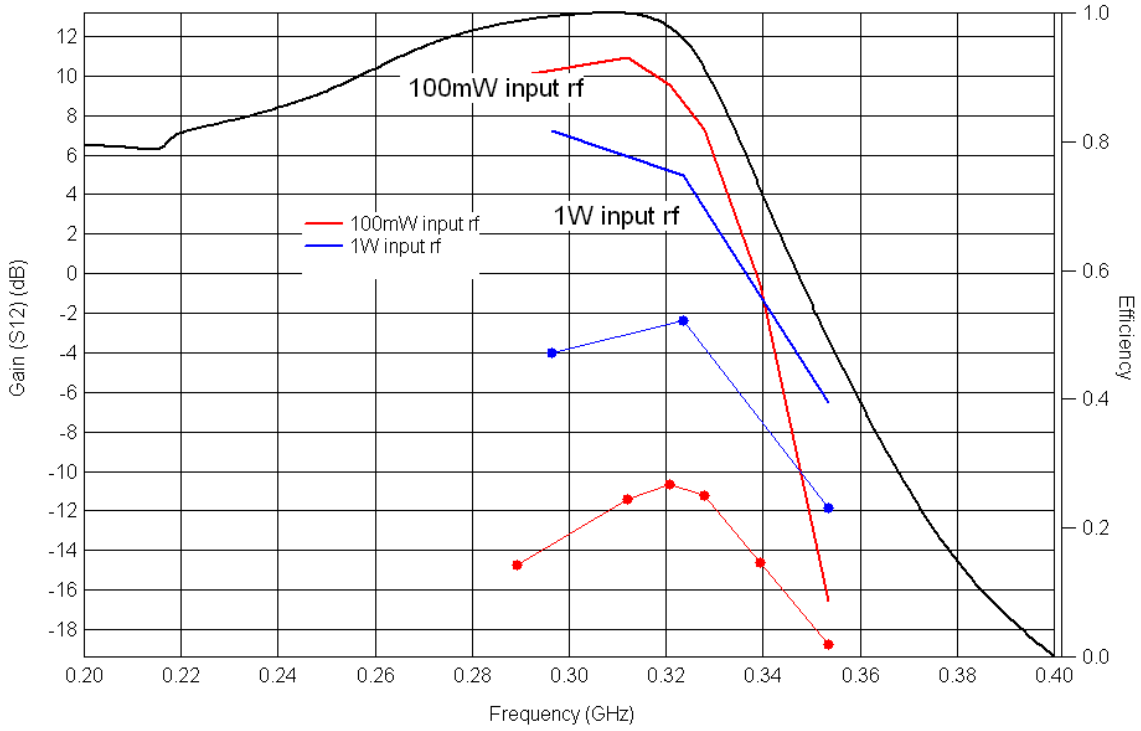

Figure 39: Efficiency and gain measurements at small signal, 1.5W, and 6W output.

In essence, the small signal based design was able to get this P/A to about three quarters of our performance goals. The part exhibited reasonable 10-13 dB gain in the lower power levels, and efficiency does get to 40-55% range, but the P/A can and should perform even better. In addition, the addition of the MEMS tuning circuits was shown in the models to compensate well for impedance variation, which could also be used to compensate for limited power differences. The design loop needs to be closed again with a rigorous large-signal design process, plus improved heat sinking, plus a Doherty architecture (or other multi-biasing approach) is needed.[8] It is clear that undertaking only one or two of these approaches will not hit target goals across the entire operating spectrum of power, environment, and impedance variance.

5. Conclusions and Future Work

The goal of this program was to develop a nanoparticle lubricant technology that improved the performance of RF MEMS switching and tuning devices to meet specifications required by tactical radios. In this program, three tasks were undertaken to achieve this goal and demonstrate the viability of the NPL, RF MEMS, and P/A tuning technologies. In the first task, a candidate NPL was modified for manufacturability and compatibility with a production MEMS packaging process. In the second task, the NPL was added to MEMS relays, which then demonstrated improvement in switching lifetime and power handling. In the third task, a radio power amplifier was designed for RF MEMS tuning, with a comparatively crude prototype demonstrating performance that exceeds present products at a fraction of the cost and size.

5.1. Task 1 Conclusions

UDRI provided NPL synthesis support for XCOM and was tasked to provide quality gold NPL material for switch lubrication. UDRI performed a review of NPL synthesis methodology and set-up a synthesis laboratory dedicated to providing material to XCOM. This included acquisition of chemicals, glassware, tubing, and other needed instruments. Numerous difficulties arose during initial synthesis attempts that prevented successful delivery of the desired material. Problems were related to solubility, cleanliness, environmental factors, and synthesis method.

Over time, fortunately, UDRI overcame these difficulties and developed a detailed synthesis method that produced an effective and stable NPL material. The NPL was transferred to toluene using a centrifuge-based extraction method that also allowed for high purity clean material, which is needed for performance in the switch application. High purity gold NPL was provided to XCOM in sufficient quantity for deposition and testing experiments on RF MEMS relays.

The toluene solvent led to a solid bridging problem in the XCOM post-processing and NPL deposition stages. UDRI investigated other surfactants and solvents through synthesis and solubility studies in an attempt to obtain a NPL in a solvent other than toluene. The Au-MES-adogen NPL in toluene was found to be the best material that we could synthesize for the XCOM switch, and so the solid bridging problem associated with toluene had to be solved in a different manner. After trial and experiment, a dip deposition and partial-dry with secondary rinse solvent proved to deliver the NPL to the contacts in a desirable quantity.

5.2. Task 2 Conclusions

In the second task, the NPL was deposited on RF MEMS die that were subsequently sealed in the standard hybrid hermetic package used in XCOM's relay products. A wet dip and partial dry process with subsequent rinse in a highly volatile solvent proved to be the best deposition method in terms of maintaining functional electromechanical yield. The process was also designed and set up for use in whole-wafer processing, although full device wafers were not used in this program due to significant cost and time over-runs in the wafer-scale packaging work.

Once the relays were packaged, sets of devices both baseline and NPL from paired lots were tested for cycle lifetime under different operating conditions. The conditions tested included 5 mW and 2 W CW RF signal load at 50 Ohms, and both cold-switching and hot-switching

conditions for each power level. The test results are summarized in the table below. The estimated baseline of the parts is shown in the Est. Baseline column, and the original goals of the program are shown in the NPL Goal column. The actual test data for the baseline parts and the NPL-enhanced relays are shown in the Baseline and NPL columns, respectively. The goals that were met or essentially met are circled in green, and the highest power cold-switch challenge is boxed in red. Overall, most parts met or exceeded expectations. The NPL parts showed a 2x to 10x lifetime improvement across the board between all four conditions, with the largest gains appearing in the most challenging test conditions of high-power hot switching.

Table 11: Summary of lifetime test data and achieved goals (after Table 9).

Specification	Conditions	Est. Baseline	**Baseline**	NPL Goal	**NPL**	Units
Cold Switched	at 40 dBm, 50 Ohm	10^4 to 10^6	-	10^8		cycles
	at 33 dBm, 50 Ohm	10^7 to 10^8	**8.4x10^7**	~4x10^8	**1.35x10^8**	cycles
	at 30 dBm, 50 Ohm	10^8 to 10^9	-	10^9		cycles
	at 7 dBm, 50 Ohm	10^8 to 10^9	**~7x10^8**	~1x10^9	**~1x10^9**	cycles
Warm Switched	at 20 dBm, 50 Ohm	10^3 to 10^4	-	10^6		cycles
	at 10 dBm, 50 Ohm	10^4 to 10^5	-	10^7		cycles
	at 7 dBm, 50 Ohm	10^4 to 10^5	**4.2x10^5**	~1x10^7	**7x10^5**	cycles
	at 0 dBm, 50 Ohm	10^5 to 10^6	-	10^8		cycles
Hot Switched	at 40 dBm, 50 Ohm	0	-	10^2		cycles
	at 33 dBm, 50 Ohm	10^2 to 10^4	**5x10^4**	~1x10^5	**2x10^5**	cycles

5.3. Task 3 Conclusions

In this task, it was determined that MEMS switching elements can enable low-loss tuning circuits suitable for an ultimate tactical radio P/A product goal. It was learned that the loss of the switches and capacitors themselves (1 Ohm) is critical for maintaining overall P/A gain and efficiency, so the technical path is appropriate at a high level. Size, cost, and level of integration for these components are reasonable, with a range of options available for commercialization.

A specific COTS GaN power transistor was identified as a good fit for the program and available at low cost. The passive and active components were procured and tested, with their models improved for subsequent P/A design. Several P/As were designed and iterated, and a simple hand-tunable P/A design was fabricated and tested as part of transistor characterization. A revised P/A showed a 40-55% PAE at a full power of 6.5 Watts, and a well behaved and predictable drop in efficiency at lower power. The insufficient output was caused by incomplete large-signal data in the model, as well as inadequate heat sinking causing a temperature rise.

Final testing provided the information needed to complete the transistor model, so the design loop is closed with a full SPICE-based model of all active and passive elements based on real data. Advanced biasing schemes such as real-time modulation and Doherty schemes can be implemented to address efficiency targets at the lower output powers.

5.4. Future Work

Early laboratory tests showed a 100x lifetime improvement in hot switching lifetime, which could have resulted in the boxed goals being met. The actual performance enhancements were an order of magnitude less than what was hoped for, which is unfortunate. It is hypothesized (and verified in a limited fashion by SEM) that many of the nanoparticles are removed in the AK225 rinse step (about three-fourths). This nanoparticle removal does not correlate to the theory of the corona, which is supposed to have a moderate adhesion to the gold contact surface. Together these facts suggest that a higher concentration sample might result in more nanoparticles remaining in the contact region after packaging, and therefore might provide a longer lifetime benefit. Alternatively, an additional surface modification to the gold contacts may result in stronger adhesion to the nanoparticles.

It is also likely that the lifetime gains may be stacked with other enhancement techniques such as multi-contact arrays and drive waveform shaping, each of which having been shown to enhance lifetime in the 10x range. The multi-contact arrays assist with hot-switch and warm-switch conditions, and the drive waveform shaping assist with cold-switch lifetime. The NPL adds to both types of conditions, and may stack well with these other techniques.

A program to complete the development and commercialization of nanotechnology-improved RF MEMS switching and tuning devices would require the following work:

1. Verify with additional microscopy the quantity of NPL in the contact region both before and after use under cold-switch and hot-switch conditions.
2. Modify concentration of NPL and deposition of NPL to meet desired nanoparticle quantity after packaging (and use).
3. Validate long-term aggregation and NPL stability inside packaged parts
4. Perform all relevant JAN tests for electromechanical relays (with semiconductor test enhancement to cover MEMS) on NPL-enhanced parts
5. Implement the contact array structure shown to enhancement of hot-switch and warm-switch lifetime (work with Ohio State Univ. for tech transfer)
6. Thicken signal traces and implement SP4T designs (as long as we are changing masks) to enable both hybrid and wafer-scale packaging of the die
7. Implement the revised wafer-scale packaging process with the new lower cost and lower risk supplier (a Sandia National Labs spinout)
8. Transfer NPL manufacturing to a commercial supplier (which may be a joint venture)
9. Develop the tuning circuit into a more robust and product-centric form (see below).

An alternative hybrid tuning component was conceived out of internal R&D work which promises a compromise between the low ESR of the integrated part and the higher capacitance of the hybrid part. As with other hybrid design, any COTS capacitor values can be selected prior to sealing, giving good design flexibility. In addition, this architecture will result in about half the overall ESR of the originally designed hybrid part, with about 1 Ohm total ESR, or 0.5 Ohms under certain conditions. This is much closer to the integrated performance level desired, and may be sufficient for a final design in production.

The circuit below uses a MEMS die to directly mate to four ultra-small 01005 chip capacitors. Two vendors have been found with these sized capacitors in values (range from 1 to 60 pF) and low ESR values (below 0.2 Ohm) suitable for the program. The first vendor is Passive Plus as previously cited, with their 01005 product line brand new and not yet available for public release. We have already secured Beta samples of these components, and they have a wide range of values up to 100 pF at 0.2 Ohms ESR through 1 GHz. The parts are 12x6x6 thousands of an inch, which will fit inside the package cavity. The second vendor is Murata, who has capacitors that are slightly smaller in size at 12x6x4 thousands of an inch, but are also not generally available yet. We do not yet have delivery time for this vendor.

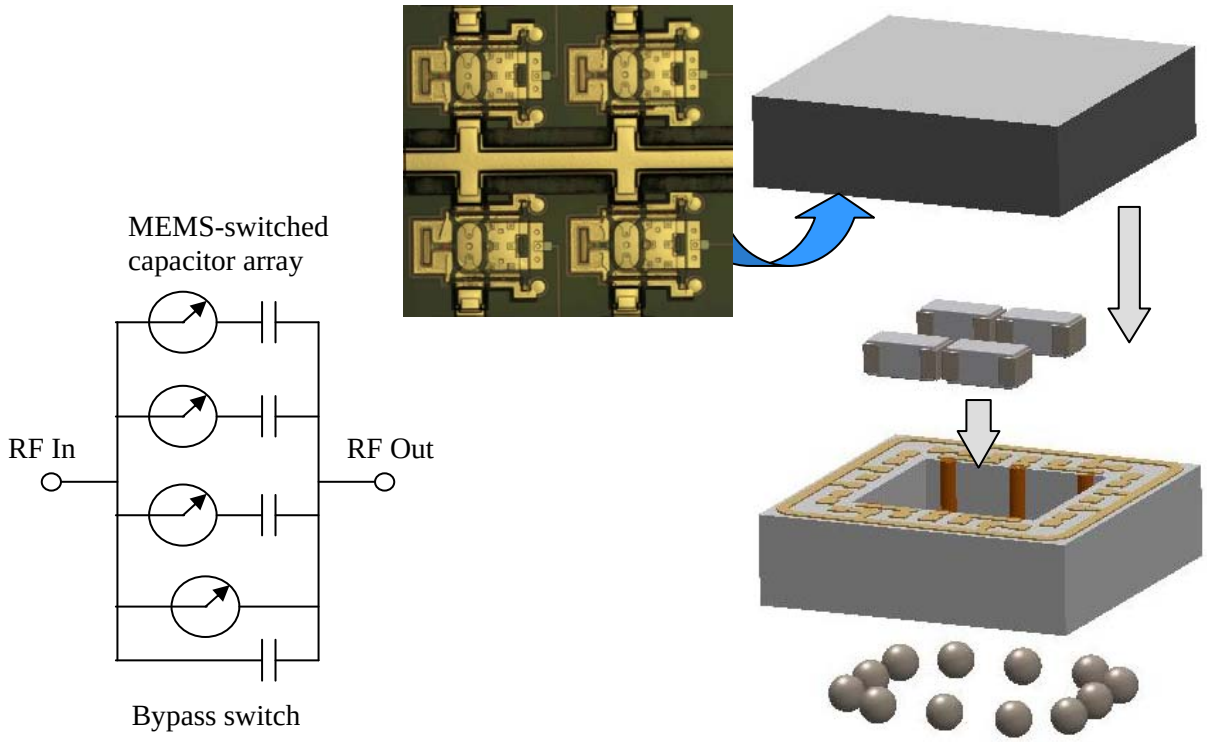

Figure 40: Circuit diagram and package architecture for novel quasi-hybrid-integrated tuner.

The entire circuit can be packaged using the new lower-cost wafer scale packaging process already in development. The two changes are that the RF MEMS wafer is first processed with the NPL as we have already proposed, but also the wafer-scale package wafer itself has thousands of the chip capacitors soldered into the head cavities across the wafer. This process must be done with an automated pick and place, and XCOM would use NexGen or AeroAntenna as suppliers for this work (both local and with modern workcells capable of 01005 handling). The bottom surface is arranged with solder balls for ease of subsequent handling and use by radio and amplifier developers.

Initial prototypes of this very novel quasi-hybrid-integrated-wafer-scale tuning circuit should be available for validation prior to any potential follow-on proposal.

6. References

1. Bourlinos, A.B., Chowdhury, S.R., Herrera, R., Jiang, D.D., Zhang, Q., Archer, L.A. and Giannelis, E.P., "Functionalized Nanostructures with Liquid-Like Behavior: Expanding the Gallery of Available Nanostructures," *Adv. Funct. Mater.*, **15** (2005) 1285-1290.
2. Itoh, H., Naka, K. and Chujo, Y., "Synthesis of Gold Nanoparticles Modified with Ionic Liquid Based on the Imidazolium Cation," *J. Am. Chem. Soc.*, **126** (2004) 3026-3027.
3. Patton, S.T., Voevodin, A.A., Vaia, R.A., Pender, M., Diamanti, S.J. and Phillips, B., "Nanoparticle Liquids for Surface Modification and Lubrication of MEMS Switch Contacts," *J. MEMS*, **17** (2008) 741-746.
4. Li, Z., Liu, Z., Zhang, J., Han, B., Du, J., Gao, Y. and Jiang, T., "Synthesis of Single-Crystal Gold Nanosheets of Large Size in Ionic Liquids,", *J. Phys. Chem. B*, **109** (2005) 14445-14448.
5. Addison, C.J. and Brolo, A.G., "Nanoparticle-Containing Structures as a Substrate for Surface-Enhanced Raman Scattering," *Langmuir*, **22** (2006) 8696-8702.
6. Zou, X.Q., Bao, H.F., Guo, H.W., Zhang, L., Li, Q., Jiang, J.G., Niu, L. and Dong, S.J., "Mercaptoethane Sulfonate Protected, Water-Soluble Gold and Silver Nanoparticles: Syntheses, Characterization and Their Building Multilayer Films With Polyaniline Via Ion-Dipole Interactions," *Journal of Colloid and Interface Science*, **295** (2006) 401-408.
7. Matsuzaki, N., Oshima, T. and Nishioka, A., "Process of extracting vegetable oil and fat," US Patent 4486353 (1984).
8. RF Power Amplifiers for Wireless Communications Artech House, Steve C. Cripps, 2006

Appendix A: RF MEMS Nanoparticle Lubricant TRL

This appendix discusses the maturity of the technologies presented in this report in terms of the DoD Technology Readiness Levels (TRLs). In brief, the technologies we developed in this work begin the program having nearly completed TRL 3. The goal of the program, from a technology maturity point of view, was to demonstrate that a NPL material could be fabricated, deposited into a MEMS switching device, and then provide improved performance benefit, which takes the technology through the technical aspects of TRL5. The relative acceleration of the technologies has been deemed of interest to multiple organizations, including Skyworks, Rockwell-Collins, and Harris Corporation.

The following charts show the critical technology and system demonstrations for each of TRLs 3 through 5. Initial status in each case is represented by an "X" in the box location. Each status that was accomplished by the end of the program effort is listed as "P". Each status that was accomplished due to other programs ongoing during the same time frame but not part of this program is listed as "R". In each case, quantification and details have been provided to a degree throughout this proposal.

TRL3: Analytical and Experimental Critical Function and/or Proof of Concept.

Active research and development is initiated. This includes analytical studies and laboratory studies to physically validate analytical predictions of separate elements of the technology. Examples include components that are not yet integrated. All were met before program start.

TRL 3 Hardware Maturity Criteria	Met[1]	Not Met[2]	N/A[3]
1. Predictions of elements of technology capability validated by: a. Analytical Studies, b. Laboratory Experiments, and/or c. Modeling and Simulation *Provide details of the studies, experiments, and M&S.*	 X X X	 ☐ ☐ ☐	 ☐ ☐ ☐
2. Scaling studies have been started. *Define the goals of the studies and how the goals relate to the overall System mission.*	X	☐	☐
3. Preliminary performance characteristics and measures have been identified and estimated. *Quantify level of performance.*	X	☐	☐
4. Cross technology effects *(if any)* have begun to be identified. *Identify other new or in development technology that could increase performance and reduce risk.*	P	☐	☐
5. Design techniques/codes have been identified and defined to the point where small applications may be analyzed/simulated.	P	☐	☐

1. For each criterion that HAS been met provide background information for verification as noted.
2. For each criterion that HAS NOT been met provide status and an estimate for meeting criteria.
3. For each criterion marked N/A provide supporting documentation for this selection.

TRL4: Component and/or Breadboard Validation in Laboratory Environment.

Basic technology components are integrated to establish that they will work together, including use of "ad hoc" hardware. This is relatively "low fidelity" compared to the eventual system.

This program concentrated on the component-level integration of the NPL technology with the RF MEMS switching technology in order to obtain performance benefits. This work is at the heart of TRL4 testing in a laboratory environment with pre-production form components and integration plans. The cross-technology issues dominated this program, and design and process techniques had to be developed to overcome these issues. In addition, technology transfer agreement discussions have begun with connection to the licensing contractor responsible for Air Force technology.

TRL 4 Hardware Maturity Criteria	**Met[1]**	**Not Met[2]**	**N/A[3]**
1. Low fidelity hardware technology "system" integration and engineering completed in a lab environment with hardware in the loop/computer in the loop tools to establish component compatibility. *Provide summary reports of efforts*	P	☐	☐
2. Technology demonstrates basic functionality in simplified environment. *Describe demonstrated functionality and provide summary of collected data.*	P	☐	☐
3. Scaling studies continued to next higher assembly from previous assessment. a. Scaling documents and diagrams of technology have been completed. b. Scalable technology prototypes have been produced. *AF mission enhancement(s) clearly defined within goals of the study.*	 P P	 ☐ ☐	 ☐ ☐
4. Integration studies have been started. *Provide ROM integration cost estimate, with Systems Engineering, Executive Officer, and user inputs & coordination.*	P	☐	☐
5. Draft hardware and software designs documented. *Provide documentation.*	P	☐	☐
6. Some software components are available. Executables are debugged, compiled and expert programmer is able to execute. *Provide documentation of efforts.*	P	☐	☐
7. Parts & components in pre-production form exist. *Provide documentation..*	P	☐	☐
8. Production and integration planning have begun. *Document planning efforts.*	P	☐	☐
9. Performance metrics have been established. *Provide performance metrics.*	P	☐	☐
10. Cross technology issues *(if any)* have been fully identified. *Document issues.*	P	☐	☐
11. Design techniques/codes have been defined to the point where medium level problems are accommodated. *Document level of fidelity and code ownership.*	P	☐	☐
12. Begin discussions/negotiations of Technology Transition Agreement to include data in items 1 through 5, 8, and 9.	P	☐	☐

The focus of the last task and much of the internal complementary research and development (and other programs) were to address the more advanced operational testing and circuit-level integration and assessment. This type of work proceeds well into TRL5, as does the more advanced modeling and demonstrations of RF MEMS-enabled tuning networks. XCOM was able to take advantage of business and manufacturing relationships to transfer the deposition process to a commercial foundry as well as bring up a lower-cost alternative for wafer-scale packaging in the next stage of commercialization.

Additional support needs to be secured from follow-on circuit development and manufacturing programs to address remaining TRL 5 and future TRL 6 & 7 tasks. The TRL improvement for NPL-enhanced relays for test equipment can be performed quickly, with qualification achievable within 12 mo. Full qualification and production of NPL-enhanced RF MEMS tuning circuits for tactical radios, however, would take an estimated 24-36 mo.

TRL5: Component and/or Breadboard Validation in Relevant Environment.
Fidelity of breadboard technology increases significantly. The basic technological components are integrated with reasonably realistic supporting elements so that it can be tested in simulated environment. Examples include "high fidelity" laboratory integration of components.

TRL 5 Hardware Maturity Criteria	Met[1]	Not Met[2]	N/A[3]
1. High fidelity lab integration of the hardware technology "system" completed and ready for testing in realistic simulated environments. *Provide summary reports of integration efforts. Define relevant environment used in testing.*	P	☐	☐
2. Preliminary hardware "system" engineering report completed that addresses: a. Performance (including how this translates to performance of final product) b. Integration c. Test and Evaluation d. Mechanical and Electrical Interfaces *Provide preliminary hardware technology "system" engineering report.*	 R R R R	 ☐ ☐ ☐ ☐	 ☐ ☐ ☐ ☐
3. Detailed design drawings have been completed. Three view drawings and wiring diagrams have been submitted.	P	☐	☐
4. Pre-production hardware available. a. Prototypes have been created. b. Processes have been reviewed with Manufacturing and Producibility office(s). *Update ROM integration cost estimate & provide schedule for user integration.*	 P ☐	 ☐ M	 ☐ ☐
5. Form, fit, and function for application has begun to be addressed in conjunction with end user development staff. *Provide details of efforts to date.*	P	☐	☐
6. Cross technology effects *(if any)* identified and established through analysis. *Provide documentation of effects.*	P	☐	☐
7. Design techniques/codes have been defined to the point where largest problems defined. *Provide details on how this technology will solve largest problems.*	R	☐	☐
8. Scaling studies continued to next higher assembly from previous assessment. *Describe scaling to new functional capability and regions of operational area.*	R	☐	☐
9. Technology Transition Agreement has been updated to reflect items 1 through 3, 5, and 8. TTA coordinated and approved by end user Executive(s) and S&T Executive following completion of applicable System management approval process.	☐	M	☐

Acronyms

1-D, 2-D, 3-D	One, Two, or Three Dimension/Dimensional (depending on usage)
AC	Alternating Current
AFB	Air Force Base
AFRL	Air Force Research Laboratory
ARO	Army Research Office
BGA	Ball Grid Array (package interface type)
C4ISR	Command, Control, Communications, Computers, Intelligence, Surveillance, and Reconnaissance
CECOM	Communications and Electronics Command
CO_2	Carbon Dioxide
CPW	Co-Planar Waveguide (transmission line architecture)
CSP	Chip-Scale Package
DARPA	Defense Advanced Research Projects Agency
dB	Decibels
DC	Direct Current
DFARS	Defense Federal Acquisitions Regulations
DoD	Department of Defense
DTIC	Defense Technical Information Center
EM	Electro Magnetic
FCC	Federal Communications Commission
FIB	Focused Ion Beam
GGB	not an acronym, proper noun for a high frequency test equipment supplier
GHz	Giga Hertz (measurement of frequency)
G/S/G	Ground-Signal-Ground spacing for a coplanar waveguide
HFSS	High Frequency Systems Simulator (commercial software package)
HP	Hewlett Packard (test electronics manufacturer)
IE3D	Not an acronym, a proper noun for a particular commercial software package
IETF	Internet Engineering Task Force
IMT	Innovative Micro Technology (XCOM foundry)
IP	Intellectual Property or Internet Protocol, depending on usage
JEDEC	Joint Electron Device Engineering Council
JTRS	Joint Tactical Radio System
JPL	Jet Propulsion Laboratory
LCC	Leadless Chip Carrier (package type)
LDV	Laser Doppler Vibrometer/Vibrometry, depending on usage
MEMS	Microfabricated Electromechanical Systems
MHz	MegaHertz, (measurement of frequency)
MIL PRF	Military Performance standard
MIL SPC	Military Specification
MRL	Manufacturing Readiness Level
MTT-S	Microwave Theory and Techniques Society Symposium
MUOS	Mobile User Objective System
NASA	National Aeronautics and Space Administration
NiCr	Nickel-Chromium (common resistor or adhesion metal layers)

QoS	Quality of Service
PCB	Printed Circuit Board
PECVD	Plasma-Enhanced Chemical Vapor Deposition
PI or P.I.	Principle Investigator
PMGI	PolyMethlGlutarImide (specific type of photoresist)
PR	PhotoResist
R&D	Research and Development
RF	Radio Frequency
RFIC	Radio Frequency Integrated Circuit
SATCOM	Satellite Communications
SBIR	Small Business Innovation Research
SEM	Scanning Electron Microscopy/Microscope/Micrograph depending on usage
SiCr	Silicon Chromium (resistive film)
Si_xN_y	Silicon Nitride (common dielectric film)
SPDT or SP2T	Single Pull Double Throw (type of relay or switching circuit)
SP6T	Single Pull, Six Throw (type of relay or switching circuit)
SPST	Single Pull Single Throw (type of relay or switching circuit)
TCA	Transformational Communications Architecture
Ti-W	Titanium-Tungsten (common adhesion metal layers)
TRL	Either the Technology Readiness Level or a Transmit-Reflect-deLay calibration technique, depending on the context
UAV	Unmanned Air Vehicle
US or U.S.	United States
USAF	United States Air Force
VNA	Vector Network Analyzer
WIN-T	Warfighter Information Network - Tactical
WLAN	Wireless Local Area Network (e.g., WiFi)
WWAN	Wireless Wide Area Network (e.g., cellular)
WPAFB	Wright-Patterson Air Force Base
XCOM	Not an acronym, but a capitalized proper noun (the contractor)